



Exploring dynamics relationship between carbon emissions and eco-environmental quality in Samarinda Metropolitan Area: A spatiotemporal approach

Ainun Hasanah ^a, Jing Wu ^{a,b,*}

^a Department of Urban and Rural Planning, School of Urban Design, Wuhan University, Wuhan 430072, China

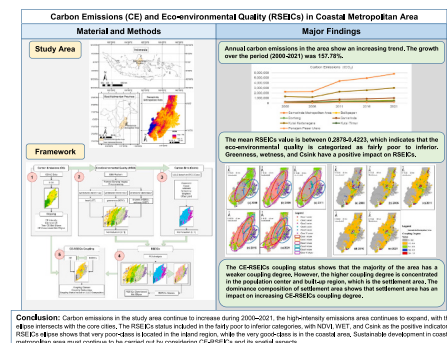
^b Hubei Habitat Environment Research Centre of Engineering and Technology, Wuhan 430072, China



HIGHLIGHTS

- This study combines CE and RSEICs by considering the spatiotemporal aspects.
- High-emission ellipse is located in the east and intersects with the core cities.
- Lower RSEICs is located in inland region, and higher RSEICs is in coastal area.
- Higher coupling degree of CE-RSEICs is concentrated in settlement area.
- Sustainable development needs to consider CE-RSEICs and its spatial aspects.

GRAPHICAL ABSTRACT



ARTICLE INFO

Editor: Pavlos Kassomenos

Keywords:

Carbon emissions
Environmental quality
Coastal region
CE-RSEICs
Coupling status

ABSTRACT

Carbon emissions have a negative impact on climate change. Environmental quality has faced significant challenges in the last decades. Eco-environmental quality helps assess the condition of the ecological environment to support humans' civilization and development. By using emissions raster dataset, remote sensing images, and LULC data, this study explores the status of carbon emissions (CE), eco-environmental quality (RSEICs), and the dynamic relationship between both variables in Samarinda Metropolitan Area, Indonesia. This study uses the spatiotemporal approach to deepen the understanding of CE-RSEICs during 2010–2021. The methods include the analysis of CE and the principal component of RSEICs. To understand the CE-RSEICs spatial features, the directional distribution ellipse method is used. Also, this study performs CE-RSEICs coupling analysis and identifies its LULC type composition. The findings show that CE status is still on an increasing trend, concentrating in the eastern region and keeping expanding during the period. The location of the low-emission ellipse is in the southwest, while the high-emission ellipse is in the east and intersects with the core cities. The mean RSEICs value is between 0.2878 to 0.4223, which indicates that the eco-environmental quality is categorized as fairly poor to inferior. Greenness, wetness, and Csink have a positive impact on RSEICs. The very poor-class ellipse is located in the inland region, and the very good-class ellipse is in the coastal area. The CE-RSEICs

* Corresponding author at: School of Urban Design, Wuhan University, Hubei Habitat Environment Research Centre of Engineering and Technology, Wuhan 430072, China.

E-mail addresses: 2021172090001@whu.edu.cn (A. Hasanah), jing.wu@whu.edu.cn (J. Wu).

coupling status shows that the majority of the area has a weaker coupling degree. However, the higher coupling degree is concentrated in the population center and built-up region, which is the settlement area. The dominance composition of settlement area in higher coupling degree shows that settlement area has an impact on increasing CE-RSEICs coupling degree. So, sustainable low carbon development in coastal metropolitan area must continue to be carried out by considering CE-RSEICs and its spatial aspects.

1. Introduction

Urbanization and industrialization are the main environmental challenges of the last decades and have made significant contributions to the climate crisis (Chandra Voumik and Sultana, 2022). These issues lead to increased carbon emissions and degradation of environmental quality. Carbon emission (CE) is mostly estimated using the IPCC methodology, but it lacks of spatial perspective of emissions distribution (Wang et al., 2020). Besides, carbon emissions growth is increasing year by year due to the changes of urban areas (Luqman et al., 2023).

In the era of sustainable development, the role of urban areas becomes very crucial. The low carbon eco-city concept is an effort to integrate humans with their natural environment through the efficient use of resources, the development of a friendly environment and sustainable economy, the formation of a harmonious society, and the project implementation that are in line with local characteristics (Yu, 2014). Sustainable development also requires the integration of ecological elements on a wider scale, such as metropolitan areas, to overcome environmental degradation in the core city and its interconnected peri-urban areas (Tache et al., 2023). Overcoming environmental problems caused by urbanization and urban expansion requires comprehensive and integrated spatial ecological planning, such as in metropolitan areas with various administrative levels below, as well as more complex natural and social aspects (Das et al., 2023).

Research on carbon emissions mostly choose macro-level and micro-level. Carbon emissions research on macro-level, including: global (Liu et al., 2022; Tian et al., 2021), regional (Acheampong et al., 2019; Bianco et al., 2019; Dogah and Awaworyi Churchill, 2022), national or country-level (Li et al., 2021; Q. Wang et al., 2023), and provincial level (Fang et al., 2019; Li et al., 2022). Studies about carbon emissions on micro-level, namely: city (Du et al., 2021; Ren et al., 2019) and smaller-scale, like rural area (Zhang and Li, 2022), even household level (Li et al., 2019). Carbon emissions research needs to be deepened on a metropolitan area scale due to the integration of cities and their surrounding areas as a result of urbanization and urban expansion, similarities in social and natural environmental aspects within metropolitan areas, and carbon emissions that are correlated and influence one another in nearby cities.

Coastal areas are critical and significant areas when it comes to climate change. At the same time, coastal regions are among the most vulnerable areas to climate change (Bukvic et al., 2020; Griggs and Reguero, 2021). There is complex relationship between land and ocean, as well as the high level of population and infrastructures in coastal regions (Yang and Li, 2023). Also, many important cities in the world are located in coastal areas (Boschken, 2013). Cities in coastal regions are often connected and integrated with each other and form a metropolitan area. Coastal metropolitan areas have a higher relationship in terms of carbon emissions and environmental quality. Carbon emissions and environmental quality have a certain relationship: coupling relationship (An et al., 2023). Carbon emissions can cause damage to the environment, while environmental degradation can influence the intensity of carbon emissions in a region.

Previous studies mostly investigated the relationship between carbon emissions and social-economic aspects (Moyer, 2023; Hasanah and Wu, 2023), industry (Griffin et al., 2016; Zhao et al., 2017), energy (Jin and Kim, 2018; Saidi and Omri, 2020), urbanization (Wang et al., 2021),

and agriculture (Chopra et al., 2022). But, there are still few studies conducted to understand the dynamic relationship between carbon emissions and eco-environmental quality. Compared to the traditional environmental quality concept, eco-environmental quality specifically represents the ability of the ecological environment to support human's lives, survival, and the development of socioeconomic sectors (Long et al., 2023).

With the technological progress of the last decades, eco-environmental quality can be represented by the remote sensing ecological index (RSEI), which has become the most widely used alternative in eco-environmental monitoring (Z. Wang et al., 2023). The use of remote sensing technology helps to monitor eco-environmental quality more effectively, quickly, and in real-time for a large scale (Z. Wang et al., 2023; Yang and Li, 2023). As a set of indexes that represent ecological conditions in a region, conventional RSEI consists of four indexes: heat, greenness, dryness, and wetness (Cao et al., 2022; Liao et al., 2023; H. Wang et al., 2023; Wang et al., 2022; Zhang et al., 2021). Model construction for the indexes is integrated by Principal Component Analysis (PCA) (Xu et al., 2019). However, in its development, RSEI has been improved and integrated with various indicators, such as: RSEILA (combined RSEI with local adaptability) (Zhu et al., 2021), MRSEI (combination of RSEI with rocky desertification index) (Ye and Kuang, 2022), A-RSEI (combination of RSEI with humidity and soil conservation) (X. Wang et al., 2023), CRSEI (improved RSEI monitoring for larger scale and longer period) (Jin et al., 2023), and RSEIFE (considering full elements of RSEI, like water bodies) (Z. Wang et al., 2023).

Cities around the world have been required to carry out sustainable development, and one of the future trends is the planning and design of low-carbon cities (X. Wang et al., 2023). Integration of the low-carbon concept with eco-environmental quality needs to be carried out to ensure that both can go hand in hand with urban development. Carbon sink within the urban sphere is significant to achieve carbon neutrality and emissions reduction (Shen et al., 2023; D. Zhao et al., 2023). Carbon sink and environmental quality can have mutual benefits or co-benefits (H. Chen et al., 2023). Also, carbon sink play an important role in balancing economic development, climate mitigation, and social-ecological sustainability (Yin et al., 2023; N. Zhao et al., 2023). A previous study tried to analyze ecological restoration based on carbon storage and eco-environmental quality as two interrelated dimensions (Yang et al., 2023). However, there is a lack of research that integrates RSEI with carbon sink and considers carbon sink as a component of eco-environmental quality. Therefore, with the background of sustainable low-carbon development and the relationship between carbon sink and environmental quality, this study proposes an approach that integrates RSEI with carbon sink, called RSEICs.

The development of Google Earth Engine (GEE) helps to process the remote sensing images for RSEI monitoring, as this platform stores many satellite data sources, such as Landsat and MODIS. At the study location during selected years, Landsat band 6 experienced an issue that resulted in Landsat data not being able to cover the entire study area, so that RSEI analysis could not be carried out with Landsat data. Therefore, MODIS data were used for this study. Besides, MODIS data was also chosen because of the routinely available data at regular intervals, the completeness of the data for a larger scale, and the availability of ready-made datasets for specific indexes: NDVI and LST. On the other hand, the carbon sink calculation is based on the LULC type in the study region.

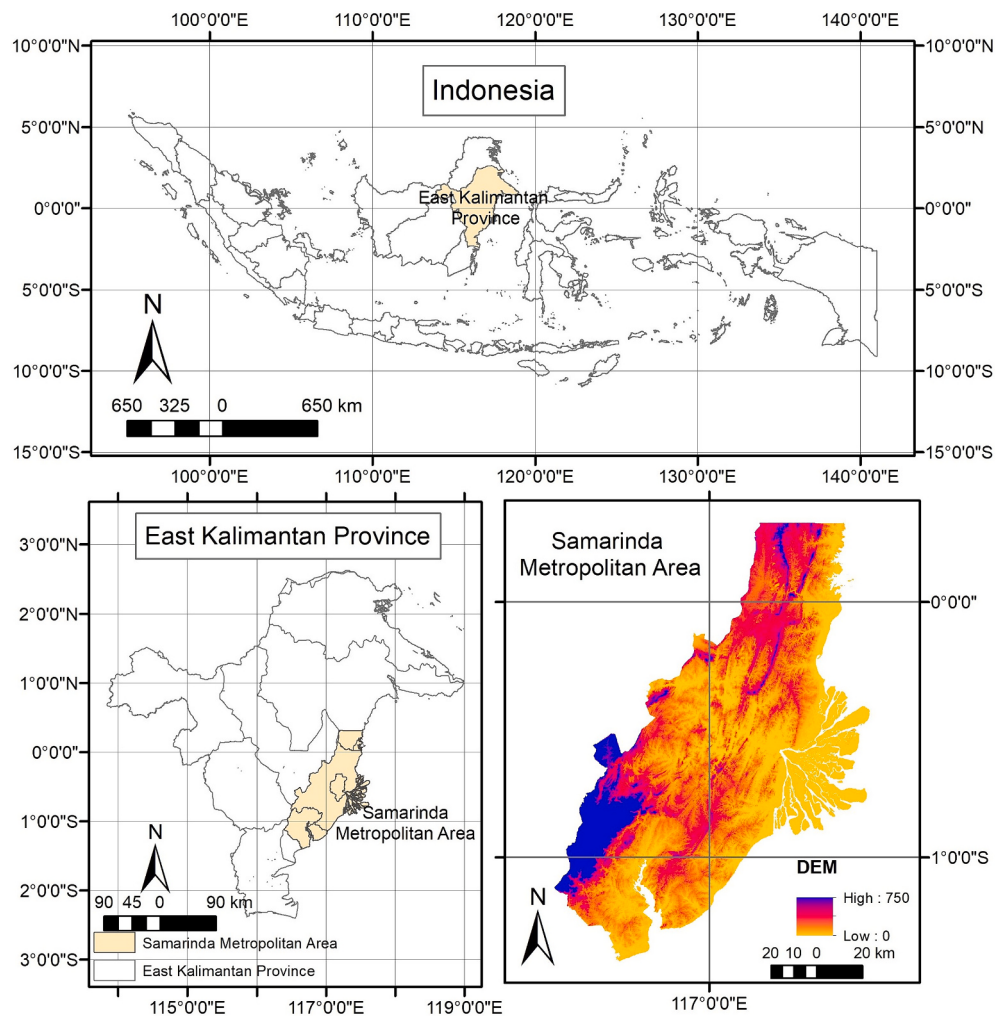


Fig. 1. Study area.

Table 1

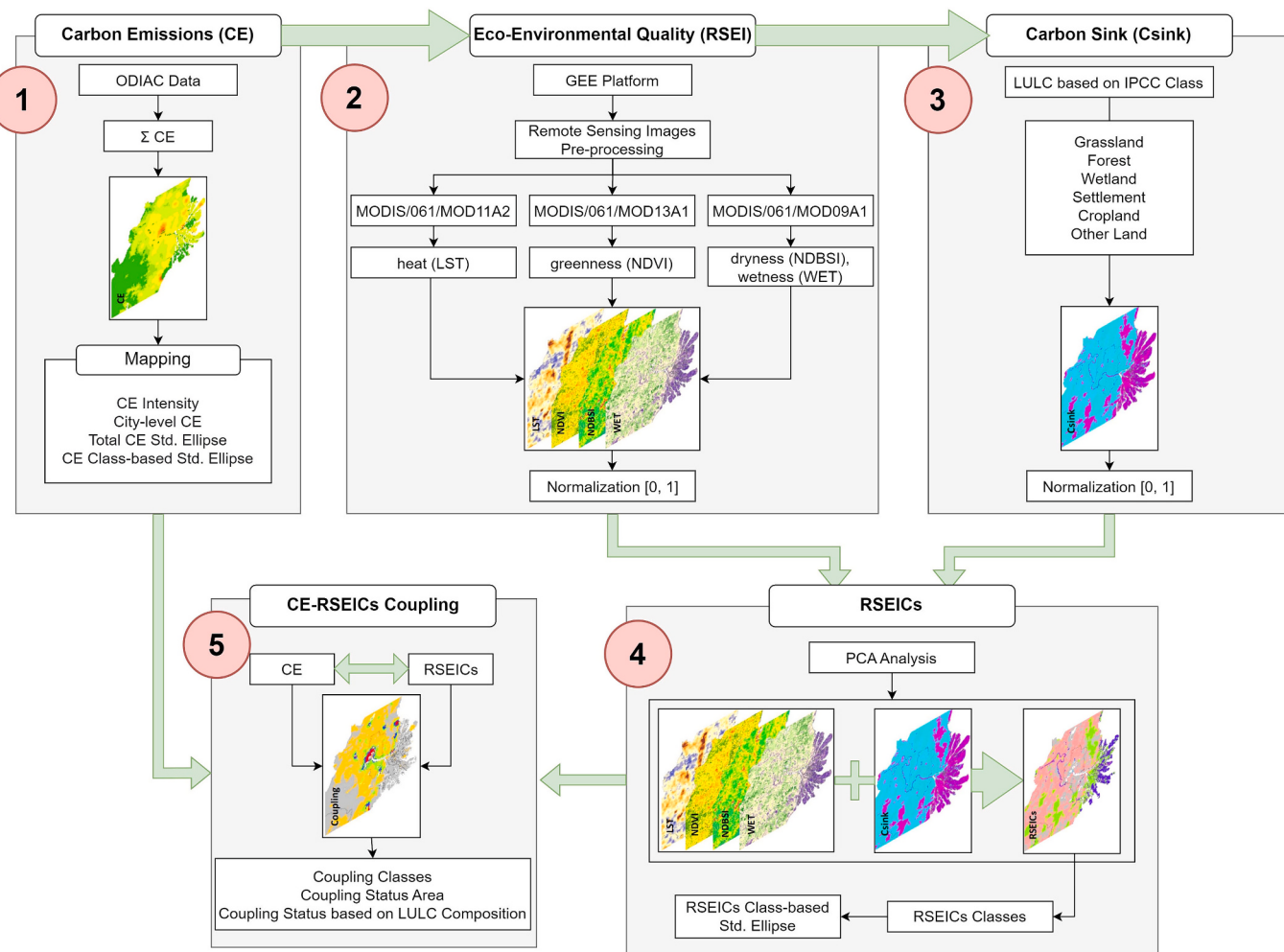
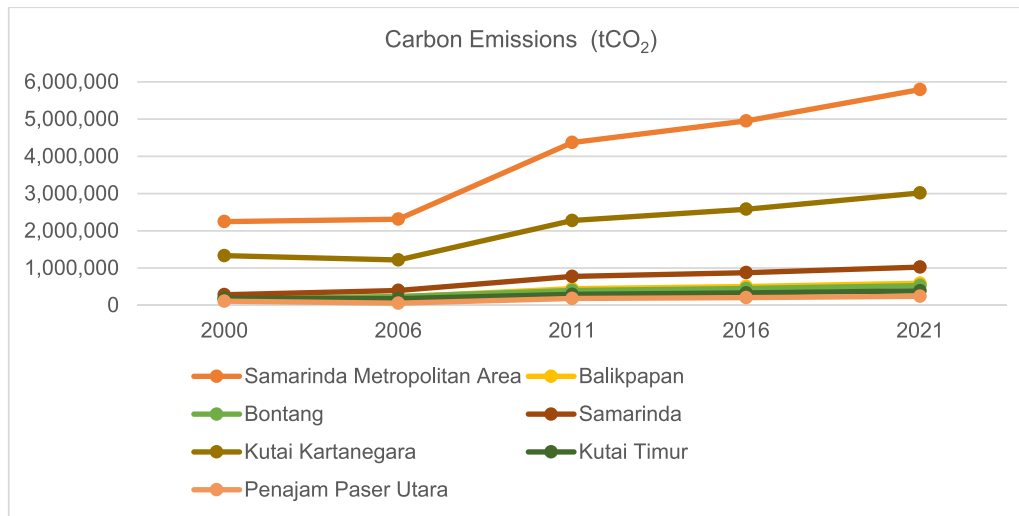
Data used in the study.

Data	Description	Source
Administrative boundary map	Multi-level Administrative Boundary	Ministry of Home Affairs
Land use/land cover (LULC) data	Reclassify based on IPCC Classes	Ministry of Environment and Forestry
Carbon emissions spatial data	Grid map 1000 m × 1000 m Based on night-time light data and power plant profile MODIS/061/MOD11A2 8-Day, 1000 m (resampled to 500 m)	https://db.cger.nies.go.jp/dataset/ODIAC/
LST (heat)	Product of land surface temperature MODIS/061/MOD13A1 16-Day, 500 m	https://developers.google.com/earth-engine/datasets/catalog/MODIS_061_MOD11A2
NDVI (greenness)	Product of vegetation index MODIS/061/MOD09A1 8-Day, 500 m	https://developers.google.com/earth-engine/datasets/catalog/MODIS_061_MOD13A1
NDBSI (dryness) WET (wetness)	Product of the surface reflectance (Bands 1–7 of Terra MODIS)	https://developers.google.com/earth-engine/datasets/catalog/MODIS_061_MOD09A1

Spatial feature of carbon emissions and eco-environmental quality need to consider, not only the distribution and the intensity, but also the trend of spatial features. Directional distribution analysis is a spatial method that can represent the centrality, direction and extent of spatial elements. The method was previously used for analysis of cultivated land patterns (Zhang et al., 2020), wildfires study (Zerbe et al., 2022), and traditional villages research (W. Chen et al., 2023). But, the use of directional distribution method in CE-RSEICs study is still minimal.

Also, there is a lack of concrete suggestions based on the existing conditions in coastal metropolitan areas from CE-RSEICs perspective and its spatial features.

Based on the problem statement and previous explanations, this study tries to fill the gaps related to the lack of integration between RSEI and carbon sink, as well as the analysis of CE-RSEICs spatial features and its dynamic relationship within a coastal metropolitan area based on the existing situations. Hence, the novelty of this study is the integration of

**Fig. 2.** Research framework.**Fig. 3.** Carbon emissions in study area during 2000–2021.

RSEI with carbon sink (RSEICs) to support low carbon development and environmental protection. Finally, the aims of this study are a) to understand the spatial and temporal characteristics of carbon emissions (CE) in the study area, b) to understand the spatial and temporal characteristics of integrated eco-environmental with carbon sink

(RSEICs) in the research area, c) to explore the dynamic relationship (coupling status) between CE-RSEICs, and d) to provide some suggestions based on the existing conditions for sustainable development in the coastal metropolitan area.

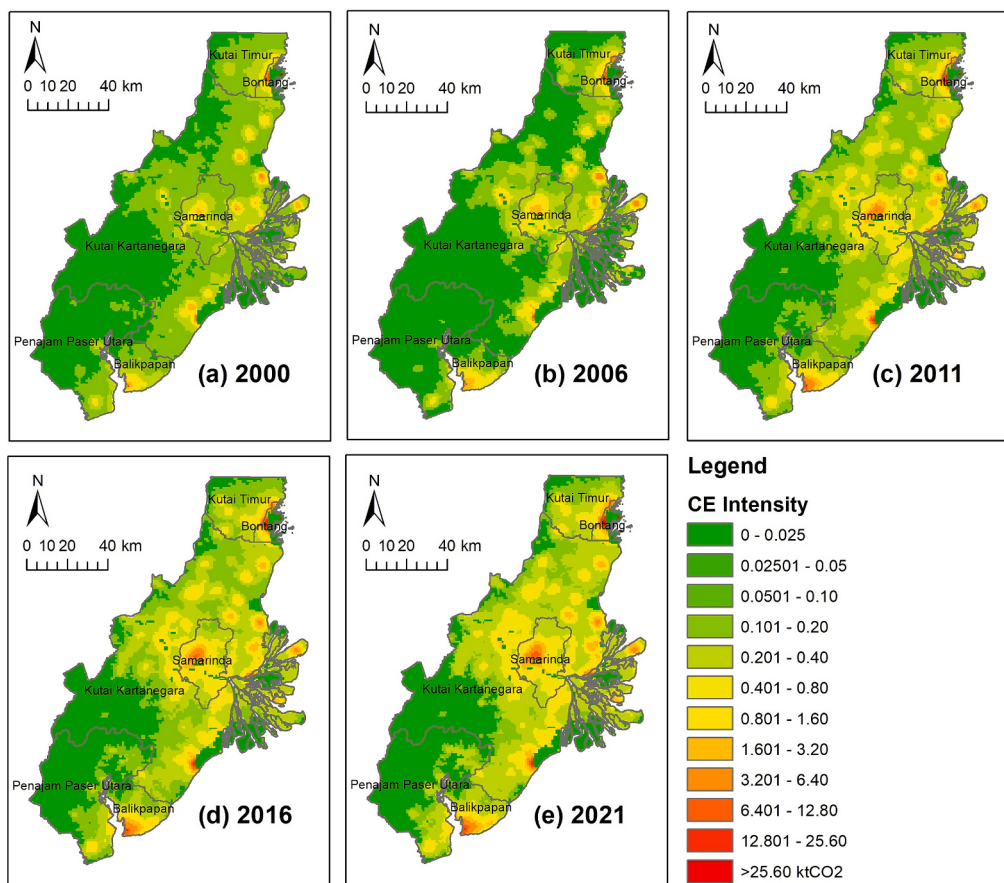


Fig. 4. Carbon emissions intensity map of Samarinda Metropolitan Area.

2. Materials and methods

2.1. Study area

Indonesia is the largest tropical-archipelago country in the world and is facing climate change challenges in many aspects. Recently, the central government of Indonesia planned to move the capital of Indonesia from Jakarta to East Kalimantan province. East Kalimantan Province is considered an ideal location for the new capital development because it is located in the central part of Indonesia. The planning of Indonesia's new capital, East Kalimantan Province, has gained more attention in recent years, especially from the perspective of urban-regional planning and development.

Samarinda Metropolitan Area is a new metropolitan area in Indonesia, located in East Kalimantan Province, and has become an important area for Indonesia's new capital development. The metropolitan area consists of six cities/municipalities and thirty-three sub-districts, including Samarinda city (the capital city of East Kalimantan province), Balikpapan city, Bontang city, parts of Kutai Kartanegara municipality, parts of Kutai Timur municipality, and parts of Penajam Paser Utara municipality. The eastern part of the Samarinda Metropolitan Area is the Makassar Strait, which makes this area a strategic coastal metropolitan area in Indonesia. The geographical location of Samarinda Metropolitan Area is 0°19' N to 1°25' S and 116°23' E to 117°38' E, with a total area of 12,372.2 km² (Fig. 1). The total population in 2021 was 2,416,673 persons. The area has typical tropical climate characteristics, with an average temperature of 27.6 °C, average humidity of 82 %, duration of sunshine of 42 %, and precipitation of 369 mm.

From environmental and land cover aspects, around 69.85 % of the Samarinda Metropolitan Area is dominated by dry shrubs, mixed dry agriculture, estate crops, secondary dryland forests, and plantation

forests. Other land covers are mining, aquaculture, and mangrove areas, respectively 6.37 %, 5.64 %, and 5.69 % of the total area. The built-up area in the Samarinda Metropolitan Area in 2021 was 553.25 km², or the equivalent of 4.47 %. From the aspect of regional development, as a buffer area for Indonesia's new capital, the Samarinda Metropolitan Area is currently facing a massive development process, including the construction of infrastructure and supporting facilities. Apart from that, moving the country's capital, followed by population movement, can also accelerate development in the surrounding areas. Massive land use change, mining activities, urban activities, and the development process of the new capital and surrounding areas can cause issues related to emissions and environmental degradation.

2.2. Data source

The data used in this study includes administrative area boundary data, land use/land cover data, carbon emissions spatial data, and remote sensing images. Administrative boundary map data was obtained from the Indonesian Ministry of Home Affairs. Land use/land cover (LULC) data was obtained from the Indonesian Ministry of Environment and Forestry. Carbon emissions spatial data was obtained from the Open-Data Inventory for Anthropogenic Carbon Dioxide (ODIAC) database. ODIAC data was obtained from the results of the analysis of satellite data (night-time light data) and statistics on power plant profiles (emission intensity and geographic location), and the products of the ODIAC data form are grid maps (1 km × 1 km) (Oda et al., 2018; Oda and Maksyutov, 2011). The ODIAC database contains emissions datasets from 2000 to 2021.

Satellite image data for Remote Sensing Ecological Index (RSEI) analysis that included the calculations of some indexes: land surface temperature (LST), normalized difference vegetation index (NDVI),

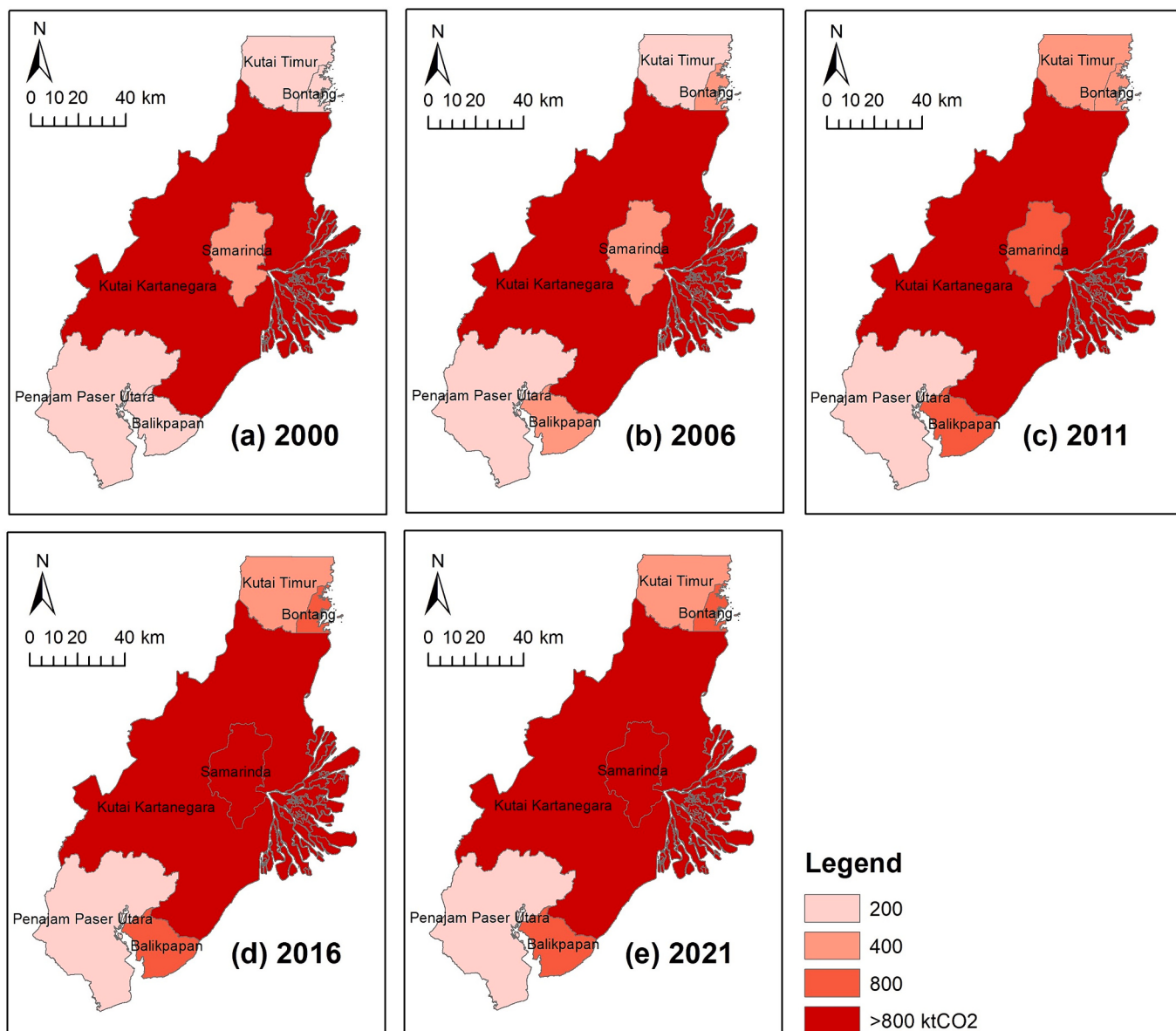


Fig. 5. City-level spatial pattern of carbon emissions in Samarinda Metropolitan Area.

normalized difference impervious surface index (NDBSI), and wetness (WET) were obtained from the Google Earth Engine (GEE) platform. The GEE platform provides MODIS data for the time period 2000–2023. The GEE code script for data acquisition of all indexes can be found in Supplementary Material S1, S2, and S3 Code Scripts. RSEICs added carbon sink indicators to eco-environmental quality analysis using LULC data. The data used in this study can be found in Table 1.

2.3. Methods

2.3.1. Carbon emissions analysis

A comprehensive and temporal national emissions database is not yet available in Indonesia, and the majority of reported country emissions monitoring results are also aggregate, sectoral, and come from existing global-regional emissions inventories from international sources (Permadi et al., 2017). Also, there is no supporting spatial emission data. Therefore, to monitor carbon emissions spatially in Indonesia, data from third parties, such as ODIAC, is really needed. ODIAC is a spatially explicit emissions inventory that has been widely used for analyzing and monitoring emissions at the global, regional, and urban levels because of

its high resolution (Oda et al., 2019). By integrating power plant profiles and satellite-observed nighttime lights, ODIAC provides a comprehensive global emissions data and timely update (Oda et al., 2018). Based on the reliability and popularity of ODIAC in emissions monitoring, as well as the limited spatial data on emissions in Indonesia, ODIAC is considered a primary data source for carbon emissions analysis in this study.

Carbon emissions analysis was calculated based on the ODIAC dataset. Yearly carbon emissions were calculated by adding up monthly carbon emissions in selected years (Yang and Li, 2023). The equation for total carbon emissions in a year is:

$$\text{CE}_{\text{year}} = \sum \text{CE}_{\text{month}} \quad (1)$$

where CE_{year} is total carbon emissions in the selected year (tCO_2) and CE_{month} is carbon emissions in each month within the selected year (tCO_2). In CE analysis, Eq. (1) was performed using Raster Calculator tool. The intensity of carbon emissions was classified into twelve classes to better visualize the emissions level spatially: green shows the lower intensity, yellow shows moderate intensity, and red shows the higher intensity of emissions (Hasanah and Wu, 2023). For city-level emissions, the Natural Breaks method in ArcMap 10.8 was performed to classify

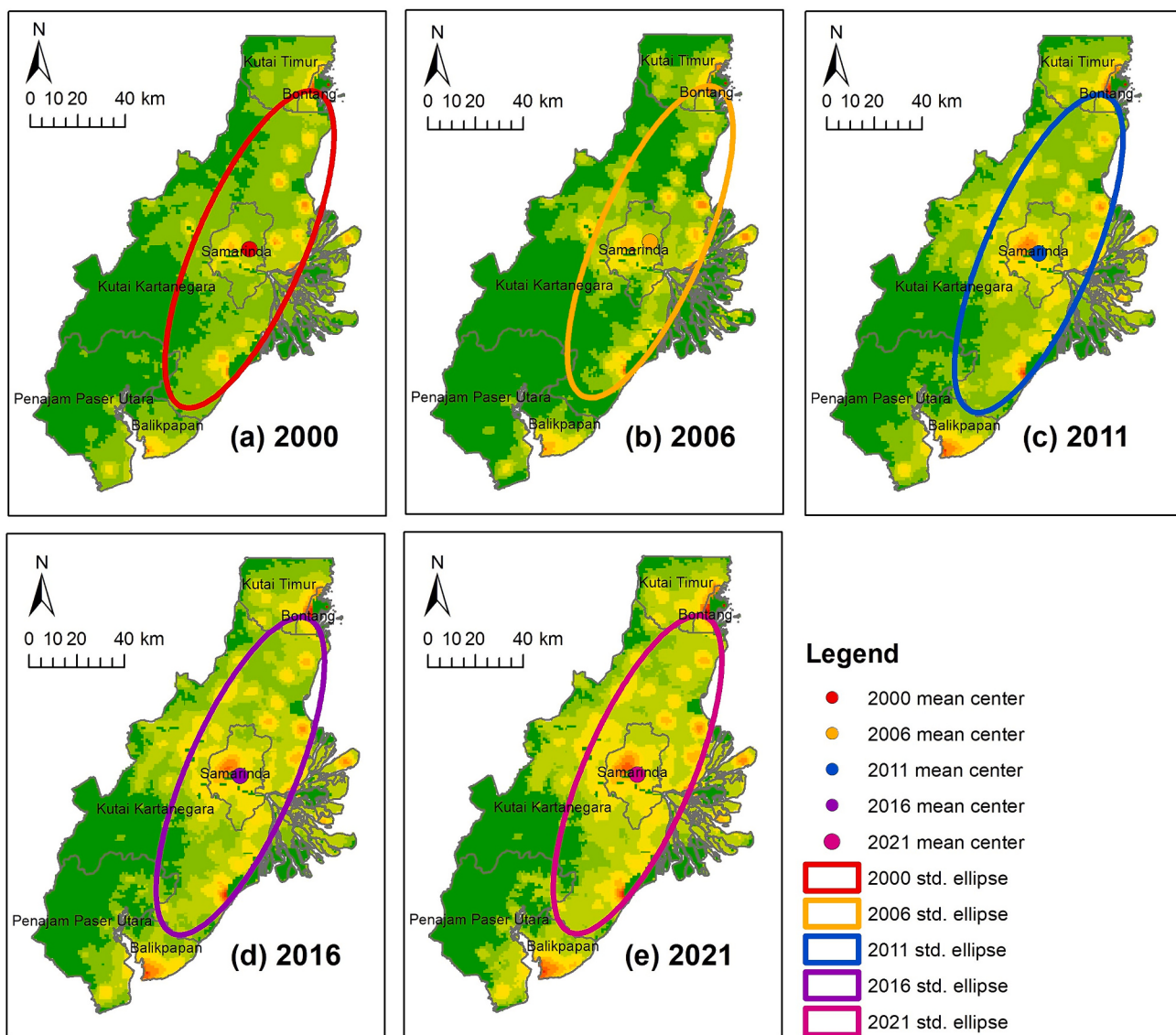


Fig. 6. Directional distribution of total carbon emissions in Samarinda Metropolitan Area.

Table 2

Directional distribution parameters of carbon emissions.

Year	X center coordinate	Y center coordinate	Rotation (°)	Area of ellipse (km ²)	Carbon emissions within ellipse (tCO ₂)	Percent of CE within ellipse (%)
2000	117.21	-0.49	23.66	5112	1,348,190.71	59.98
2006	117.22	-0.47	23.51	4947	1,400,125.25	60.52
2011	117.18	-0.51	23.54	5102	2,430,893.02	55.60
2016	117.18	-0.51	23.54	5102	2,752,655.12	55.60
2021	117.18	-0.51	23.54	5101	3,222,029.81	55.61

total carbon emissions in each city or municipality into: low (0–200 ktCO₂), medium-low (200–400 ktCO₂), medium-high (400–600 ktCO₂), and high (>800 ktCO₂) classes. Additionally, standard deviational ellipse of CE was divided into several classes: low emission (0–100 tCO₂), low-moderate emission (100–400 tCO₂), moderate emission (400–1600 tCO₂), high-moderate emission (1600–6400 tCO₂), and high emission (6400–135000 tCO₂).

2.3.2. Eco-environmental quality analysis

Eco-environmental quality is represented by the remote sensing ecological index (RSEI). RSEI is mainly calculated using four spatial indicators: heat (LST), greenness (NDVI), dryness (NDBSI), and wetness

(WET) (Hu and Xu, 2018; Jin et al., 2023; Xu et al., 2019). Since this study used MODIS/061/MOD11A2 and MODIS/061/MOD13A1, the values of LST and NDVI were directly extracted from the datasets (Supplementary Material Code Script S1 and S2). Using the MODIS/061/MOD09A1 dataset, the values of NDBSI and WET were calculated based on the following equations:

Calculation formula for dryness index (Eq. (2)), with building index and soil index calculations in Eq. (3) and Eq. (4) (Hu and Xu, 2018; Zhu et al., 2022):

$$\text{NDBSI} = \frac{\text{IBI} + \text{SI}}{2} \quad (2)$$

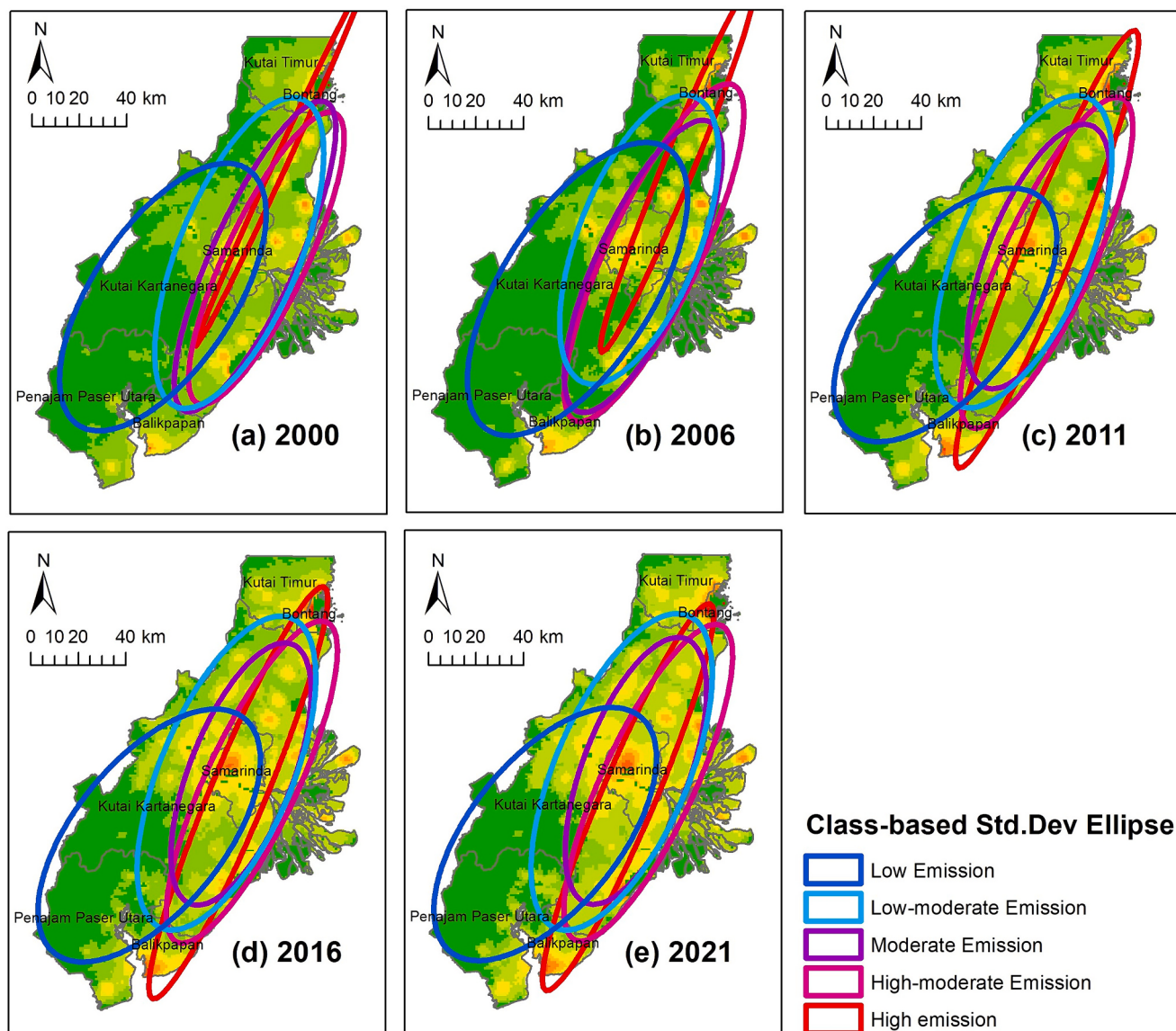


Fig. 7. Directional distribution of carbon emissions classes in Samarinda Metropolitan Area.

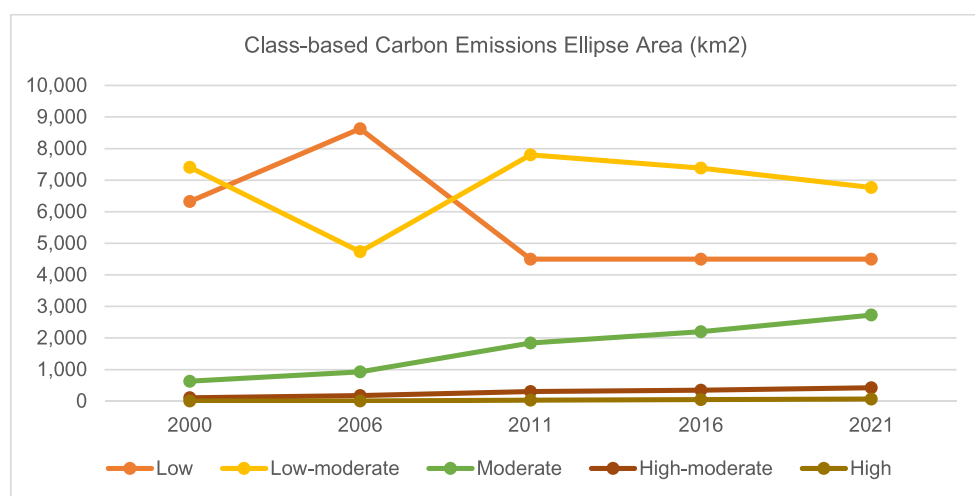


Fig. 8. Class-based carbon emissions ellipse area.

Table 3

Means of RSEICs and weight value of PC1.

Year	Means RSEICs	Weight value of PC1 indicators				
		LST	NDVI	NDBSI	WET	Csink
2000	0.4223	-0.01879	0.02976	-0.01481	0.02304	0.99901
2006	0.2944	-0.01561	0.00137	-0.02132	0.09050	0.99555
2011	0.2878	-0.04113	0.00909	-0.06775	0.08992	0.99275
2016	0.2977	-0.05199	0.02157	-0.07033	0.10993	0.98985
2021	0.3606	-0.07262	0.02687	-0.07832	0.10296	0.98857

Calculation formula for building index:

$$\text{IBI} = \frac{\frac{2\rho_{\text{SWIR1}}}{\rho_{\text{SWIR1}} + \rho_{\text{NIR}}} - \left[\frac{\rho_{\text{NIR}}}{\rho_{\text{NIR}} + \rho_{\text{pred}}} + \frac{\rho_{\text{green}}}{\rho_{\text{green}} + \rho_{\text{SWIR1}}} \right]}{\frac{2\rho_{\text{SWIR1}}}{\rho_{\text{SWIR1}} + \rho_{\text{NIR}}} + \left[\frac{\rho_{\text{NIR}}}{\rho_{\text{NIR}} + \rho_{\text{pred}}} + \frac{\rho_{\text{green}}}{\rho_{\text{green}} + \rho_{\text{SWIR1}}} \right]} \quad (3)$$

Calculation formula for soil index:

$$\text{SI} = \frac{[(\rho_{\text{SWIR1}} + \rho_{\text{pred}}) - (\rho_{\text{NIR1}} + \rho_{\text{blue}})]}{[(\rho_{\text{SWIR1}} + \rho_{\text{pred}}) + (\rho_{\text{NIR1}} + \rho_{\text{blue}})]} \quad (4)$$

Calculation formula for wetness index (Lobser and Cohen, 2007):

$$\begin{aligned} \text{WET} = & 0.1147 \rho_{\text{red}} + 0.2489 \rho_{\text{NIR1}} + 0.2408 \rho_{\text{blue}} \\ & + 0.3132 \rho_{\text{green}} - 0.3122 \rho_{\text{NIR2}} - 0.6416 \rho_{\text{SWIR1}} - 0.5087 \rho_{\text{SWIR2}} \end{aligned} \quad (5)$$

where IBI is building index; SI is soil index; ρ_{red} , ρ_{NIR1} , ρ_{blue} , ρ_{green} , ρ_{NIR2} , ρ_{SWIR1} , and ρ_{SWIR2} represent bands 1–7 of MODIS/061/MOD09A1, respectively. The calculation processes for NDBSI and WET were performed using Google Earth Engine (GEE) (Supplementary Material Code Script S3).

In this study, the eco-environmental quality analysis includes carbon sink as an indicator. Carbon sink is closely related to the environmental conditions of an area, especially regarding land use and land cover. In other words, carbon sink capacity is strongly influenced by environmental conditions (Zhang et al., 2022). Environmental sustainability can be achieved by reducing carbon emissions and increasing carbon sinks through ecological restoration and vegetation area rehabilitation (Raihan and Tuspeko, 2022; Wu et al., 2023). These efforts can directly or indirectly impact biodiversity preservation and ecosystem resilience in the midst of the climate crisis (Buotte et al., 2020). Therefore, the reciprocal relationship between environmental quality and carbon sink is the reason behind the selection of carbon sink as an indicator for eco-environmental quality analysis in carbon research.

The integration of conventional RSEI with carbon sink is called

RSEICs. The carbon sink calculation is carried out by multiplying the sink factor based on previous studies for various types of land cover (Hasanah and Wu, 2023; Xia et al., 2019):

Calculation formula for carbon sink:

$$\text{CS}_q = k_q S_q \quad (6)$$

where CS_q is carbon sink (kg C), k_q is sink factor ($\text{kg C/m}^2 \cdot \text{yr}$), and S_q is the total area of land cover q (m^2). Because all data for RSEI analysis is in the form of a raster grid map (500 m × 500 m), the carbon sink map was also converted to the same format and in units of t/grid. Sink factors for various types of land cover: forest (16.425 t/grid), wetland (14.175 t/grid), grassland (1.15 t/grid), and cropland (0.175 t/grid). Meanwhile, the value of settlement and other land cover types was set to 0, because these land cover types are emitters rather than sinks. Because the value of the indicators was varied, all the values were normalized to [0, 1] before the next step.

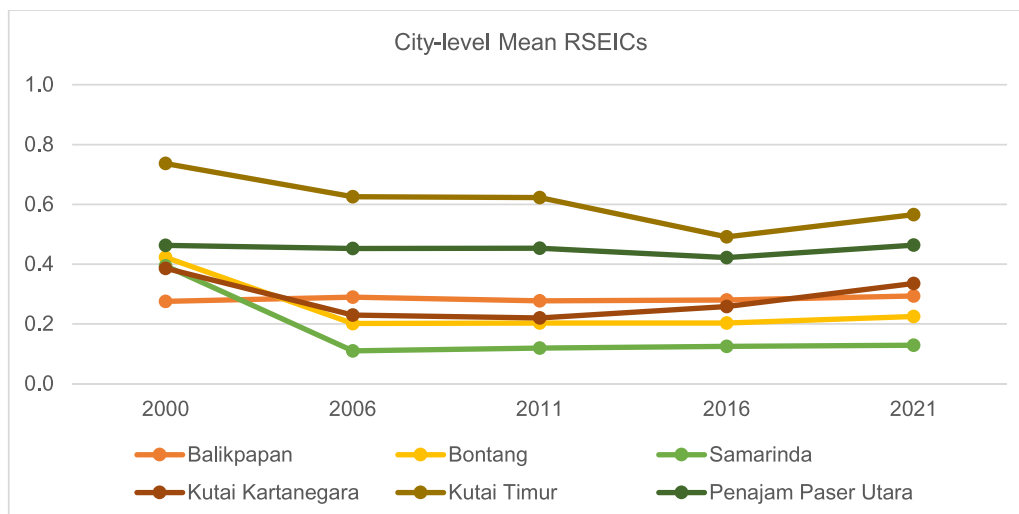
By adopting the previous RSEI calculation procedures, RSEICs also used principal component analysis (PCA) to determine the effect of each indicator on RSEICs, and the RSEICs value was normalized [0, 1]. The normalized value of RSEI represents the quality of the eco-environment in the region. The higher the value, the better the eco-environmental condition (Z. Wang et al., 2023). In other words, 0 represents very bad eco-environmental quality, while 1 indicates excellent eco-environmental quality (Xu et al., 2018). Based on previous studies, the grouping of RSEI values uses an interval of 0.2, and the purpose of classification into five classes is to create tiered levels (lowest, middle, highest, and in between) that can represent the quality of the eco-environment (An et al., 2023; Jin et al., 2023; Xu et al., 2018, 2019; Yue et al., 2019). However, in this context, to make more detail classification of RSEICs value and better represent the status of eco-environmental quality, the RSEICs was classified into ten classes with an interval of 0.1: very poor (0–0.1), poor (0.1–0.2), fairly poor (0.2–0.3), fair (0.3–0.4), inferior (0.4–0.5), moderate (0.5–0.6), moderately good (0.6–0.7), good (0.7–0.8), very good (0.8–0.9), and excellent (0.9–1.0).

RSEICs was calculated using Principal component analysis (PCA) as follows:

$$\text{RSEICs} = f(\text{LST}, \text{NDVI}, \text{NDBSI}, \text{WET}, \text{Csink}) \quad (7)$$

The normalization of RSEICs value:

$$N = \frac{I - I_{\min}}{I_{\max} - I_{\min}} \quad (8)$$

**Fig. 9.** City-level mean RSEICs in Samarinda Metropolitan Area.

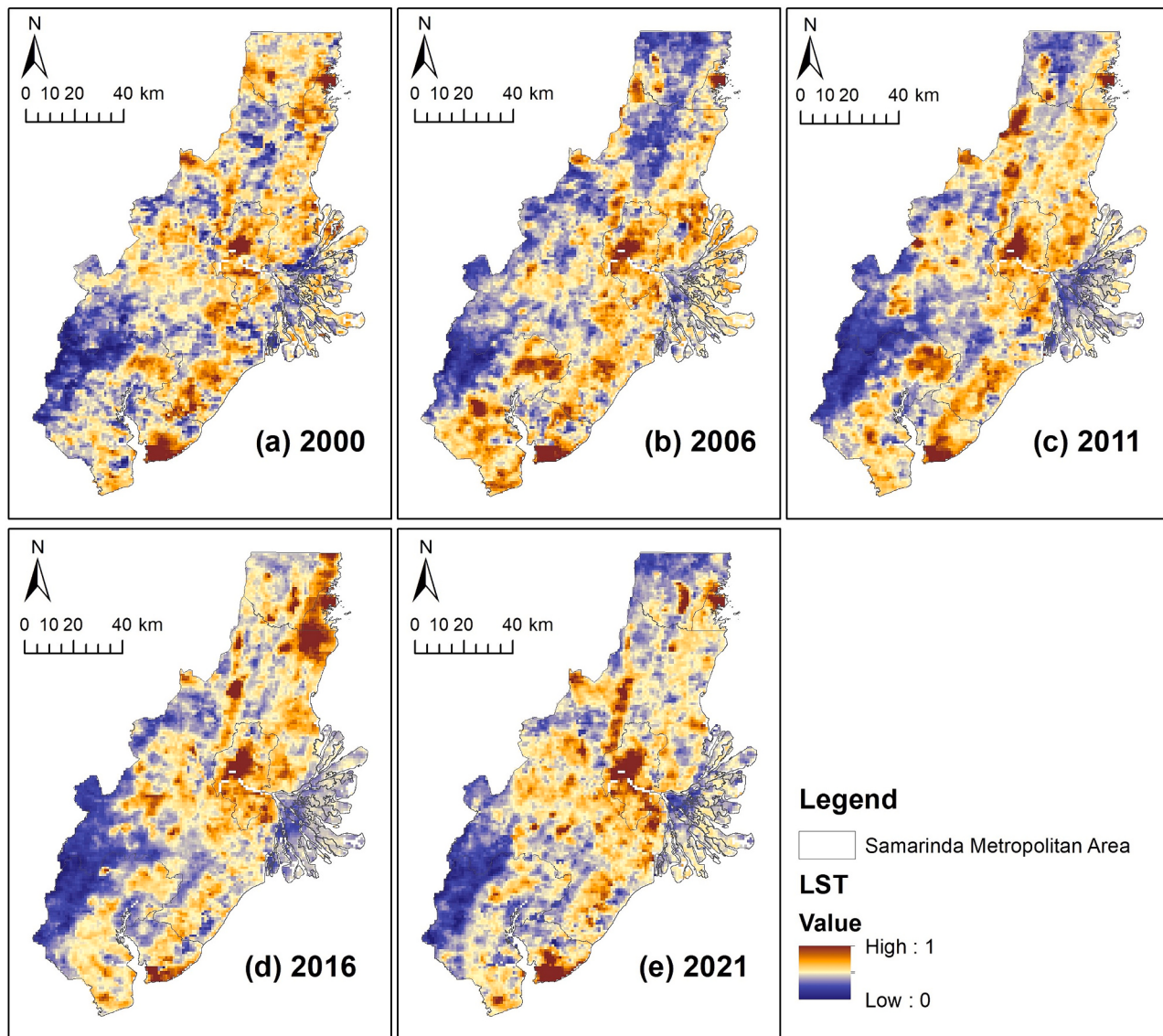


Fig. 10. Spatial distribution of LST in 2000, 2006, 2011, 2016, and 2021.

where N is the normalized version of index; I represents the actual index; and I_{\min} and I_{\max} represent the minimum and maximum values of the actual index. The analysis and map visualization of eco-environmental quality were performed in ArcMap 10.8.

2.3.3. Directional distribution analysis

Analysis of directional distribution (standard deviational ellipse) is a spatial method to understand the trend of spatial features and distribution: centrality, orientation or direction, and spatial extent (W. Chen et al., 2023; Zerbe et al., 2022; Zhang et al., 2020). The ellipse provides an estimation of the core area (Fischer et al., 2010). The parameters of consideration in directional distribution analysis include: center X coordinate, center Y coordinate, X-axis length, Y-axis length, and azimuth (rotation). Directional distribution analysis was performed in ArcMap 10.8 using the Directional Distribution (Standard Deviational Ellipse) function. Directional distribution analysis is used to understand the nature of both carbon emissions and eco-environmental quality. The equations of the standard deviational ellipse and the components are as follows (W. Chen et al., 2023):

Calculation formula of X mean center of the ellipse:

$$X = \frac{\sum_{i=1}^n w_i x_i}{\sum_{i=1}^n w_i} \quad (9)$$

Calculation formula of Y mean center of the ellipse:

$$\bar{Y} = \frac{\sum_{i=1}^n w_i y_i}{\sum_{i=1}^n w_i} \quad (10)$$

Calculation formula of standard deviation X-axis:

$$SDE_x = \sqrt{\frac{\sum_{i=1}^n (y_i - X)^2}{n}} \quad (11)$$

Calculation formula of standard deviation Y-axis:

$$SDE_y = \sqrt{\frac{\sum_{i=1}^n (x_i - \bar{Y})^2}{n}} \quad (12)$$

Calculation formula of rotation of the ellipse:

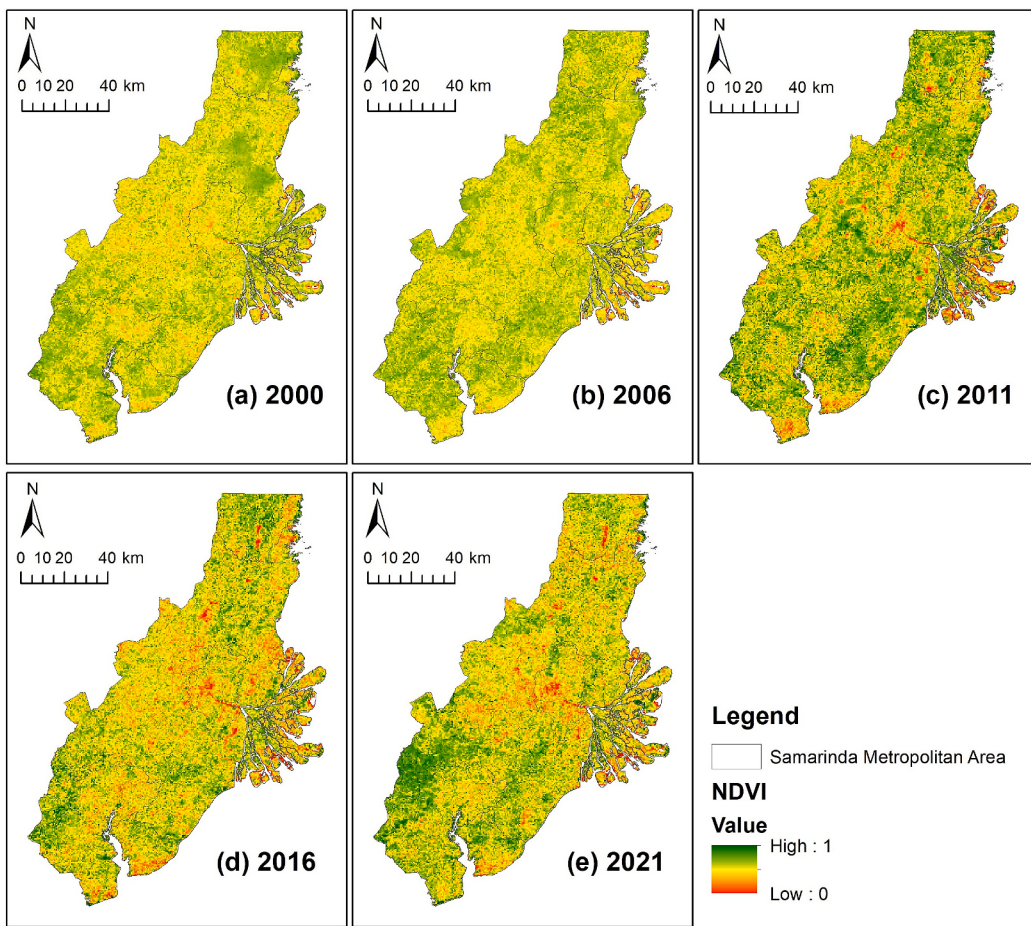


Fig. 11. Spatial distribution of NDVI in 2000, 2006, 2011, 2016, and 2021.

$$\tan \theta = \frac{\left(\sum_{i=1}^n \tilde{x}_i^2 - \sum_{i=1}^n \tilde{y}_i^2 \right) + \sqrt{\left(\sum_{i=1}^n \tilde{x}_i^2 - \sum_{i=1}^n \tilde{y}_i^2 \right) + 4 \left(\sum_{i=1}^n \tilde{x}_i \tilde{y}_i \right)^2}}{2 \sum_{i=1}^n \tilde{x}_i \tilde{y}_i} \quad (13)$$

where \bar{X} and \bar{Y} are the mean center; SDEx and SDEy are the length of the X- and Y-axes; and θ is the rotation or azimuth of the ellipse.

Each parameter can describe the spatial perspective of geographical features. The center of the ellipse, represented by X and Y coordinates, was calculated by the mean center, which can indicate the center of the concentration of the spatial features. In this context, the longer the X-axis, the greater the dispersion, while the longer the Y-axis, the more obvious the orientation. The azimuth shows the rotation (clockwise) or direction of the main trend of the spatial features. In addition, standard deviational ellipse analysis can be applied to each class, both for carbon emissions and eco-environmental quality.

2.3.4. Coupling analysis of carbon emissions and eco-environmental quality

The interaction between carbon emissions and eco-environmental quality can be seen from the coupling state. In this context, the calculation of the coupling degree was done using the following equation (An et al., 2023; Li et al., 2023; Tang et al., 2021; X. Wang et al., 2023):

$$C = \sqrt{\frac{(U \times E)}{\left[\frac{U+E}{2} \right]^2}} \quad (14)$$

where C represents the coupling degree between carbon emissions and eco-environmental quality; U is the carbon emissions value that has been

normalized; and E represents the eco-environmental quality. Coupling coordination degree was classified into five classes (X. Wang et al., 2023): 0–0.2 (weak coupling), 0.2–0.4 (slight weak coupling), 0.4–0.6 (barely balance), 0.6–0.8 (slight strong coupling), and 0.8–1.0 (strong coupling).

The coupling status map was generated using CE and RSEICs maps. Eq. (14) was performed using the Raster Calculator tool to obtain the coupling degree value and map. After calculation and analysis, the coupling status map for the study area in the selected years was visualized based on five classes in equal interval.

2.4. Research framework

The research framework of this study can be seen in Fig. 2.

3. Results

3.1. Status of carbon emissions in Samarinda Metropolitan Area

Cumulatively, the annual carbon emissions in the study area show an increasing trend (Fig. 3). The lowest emission was in 2000 with total emissions of 2,247,811.94 tCO₂, while the highest was in 2021 with total emissions of 5,794,486.55 tCO₂. Carbon emissions in the Samarinda Metropolitan Area experienced a significant increase during 2006–2011, from 2,313,673.53 tCO₂ to 4,371,899.60 tCO₂. In East Kalimantan province, the land and natural resource-based sectors (plantations, agriculture, forestry, and mining) emerged as the leading sectors. However, in that period also witnessed forest degradation caused by illegal logging and the expansion of the agricultural sector.

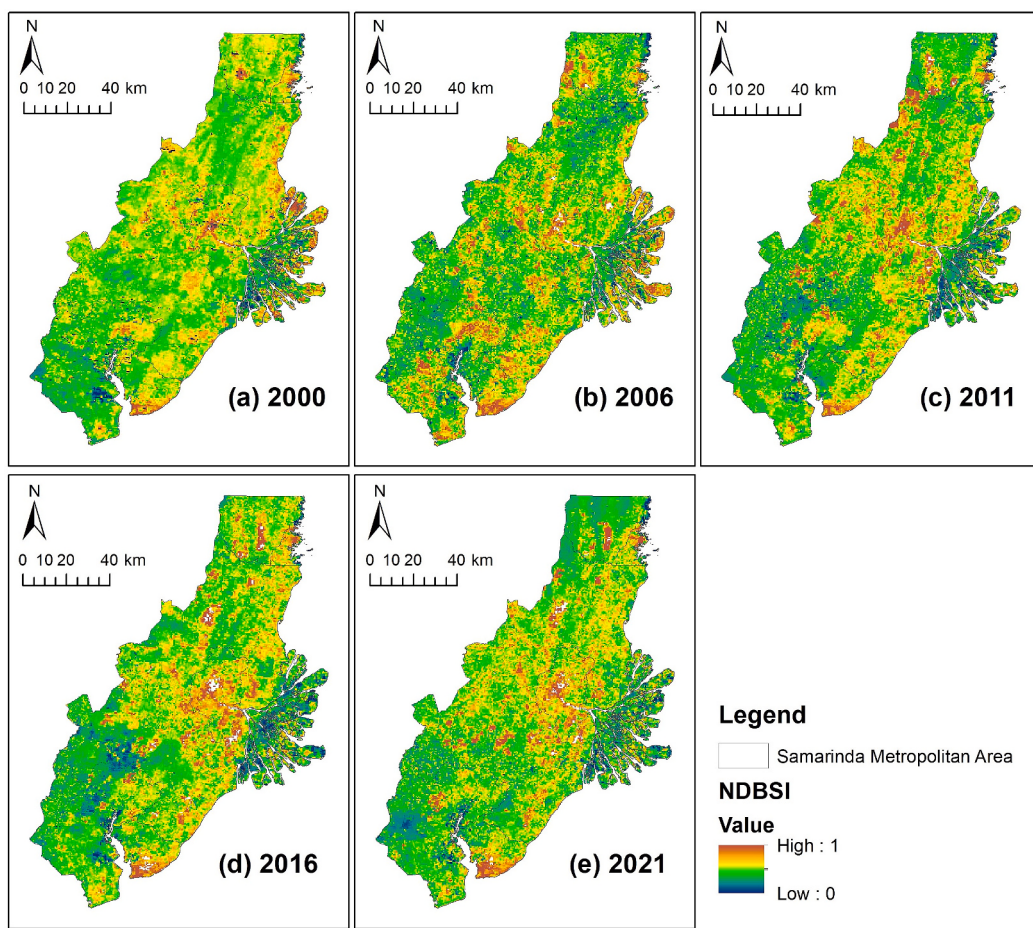


Fig. 12. Spatial distribution of NDBSI in 2000, 2006, 2011, 2016, and 2021.

These activities contributed to a significant increase in emissions during the period. The growth of carbon emissions in the Samarinda Metropolitan Area in the selected years was: 2000–2006 (2.93 %), 2006–2011 (88.96 %), 2011–2016 (13.24 %), 2016–2021 (17.04 %), and carbon emissions growth over the period 2000–2021 was 157.78 %.

At the city-level, the status of carbon emissions in six cities/municipalities showed different trends (Fig. 3). The highest contributor of carbon emissions in the study area during 2000–2021 was Kutai Kartanegara municipality, which has the largest area in the study region. The second-highest contributor was Samarinda City, as the capital of East Kalimantan Province. Balikpapan and Bontang were the third and fourth contributors, as the core cities in the region. During 2000–2021, Kutai Timur was in the fifth position, and Penajam Paser Utara municipality was the lowest contributor of carbon emissions in the region.

3.2. Spatial pattern and distribution of carbon emissions in Samarinda Metropolitan Area

3.2.1. Carbon emissions intensity

Fig. 4 is the carbon emissions intensity map of the Samarinda Metropolitan Area. Based on the intensity map, carbon emissions in the Samarinda Metropolitan Area are mostly concentrated in the areas that are relatively developed, like the downtown area, such as Samarinda City, Balikpapan City, and Bontang City. The intensity of emissions showed an increasing trend from 2000 to 2021, which means the yellow and red areas were expanding from time to time. The center of the intensity was mostly in the eastern part of the study area, which is also along the coast. In contrast, the southwest region of the Samarinda Metropolitan Area was relatively in constant status, having a green area

(lower emissions) in each selected year. This situation is influenced by the higher elevation, the natural conditions, and the lack of development in the region.

3.2.2. Spatial pattern of carbon emissions

Fig. 5 shows the spatial pattern of carbon emissions at city-level in 2000, 2006, 2011, 2016, and 2021. The spatial pattern shows the changes in city-level emissions status during the period. In 2000, there were four cities and municipalities that were included in the low-class (Penajam Paser Utara, Balikpapan, Kutai Timur, and Bontang), Samarinda City in the medium-low class, and Kutai Kartanegara in the high-class. During 2011–2021, there were significant changes in the status of each class compared to 2000 and 2006. Penajam Paser Utara was the only one included in the low-class. Kutai Timur was in the medium-low class. Balikpapan and Bontang were included in the medium-high class, while Samarinda and Kutai Kartanegara were included in the high-class. Changes in carbon emissions' spatial pattern in the study area have increased to the higher classes in recent years. The shift towards higher emissions status indicates there was rapid development in core cities and surrounding areas within the region.

3.2.3. Directional distribution of carbon emissions

The distribution of carbon emissions was reflected by a standard deviation ellipse to understand the nature of carbon emissions in the region. Fig. 6 shows the standard deviation ellipse of total carbon emissions in the study area in selected years. Table 2 describes the parameters of directional distribution in selected years. Carbon emissions in 2011, 2016, and 2021 have the same center location, that indicates no changes in the CE center in those years. The rotation of the ellipses that

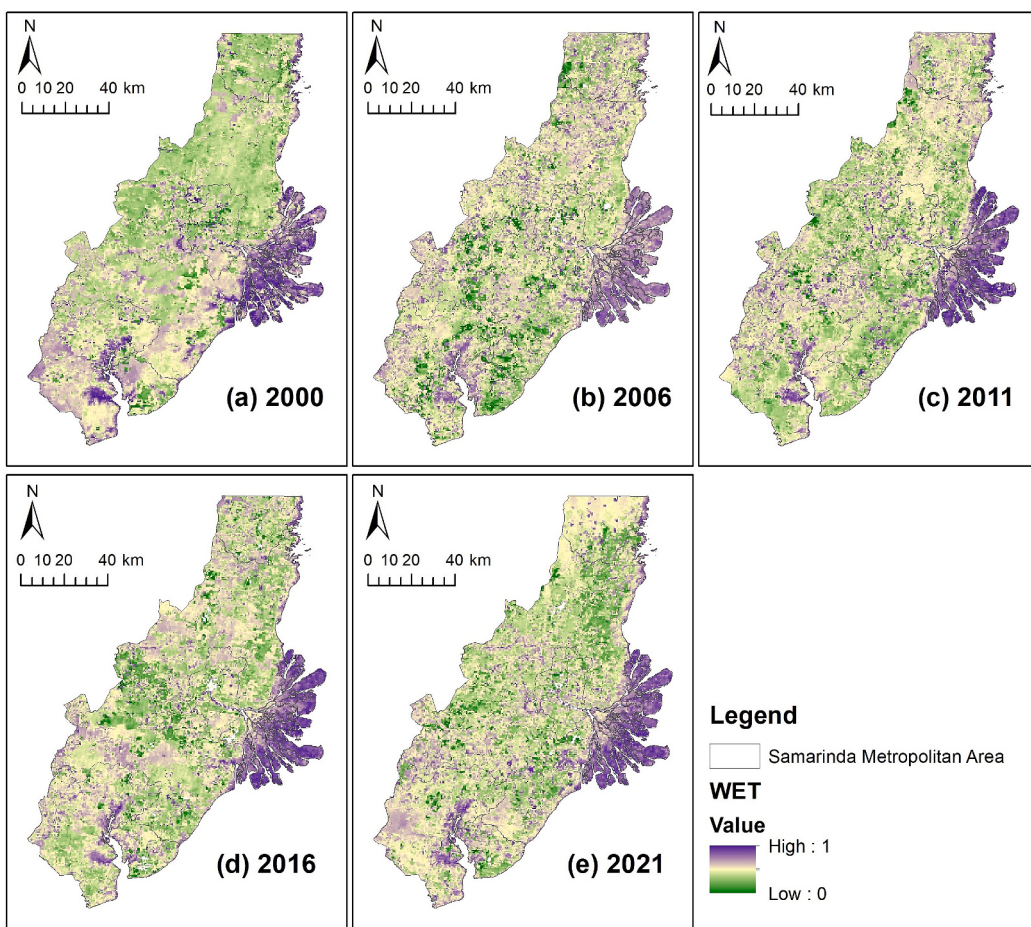


Fig. 13. Spatial distribution of WET in 2000, 2006, 2011, 2016, and 2021.

indicate the direction of emissions in selected years is also relatively constant, ranging from 23.51° to 23.66° . In 2000, the overall area of the ellipse was 5112 km^2 . However, by 2006, it had reduced to 4947 km^2 , representing a decline of 3.23 %. In 2011, the area of the ellipse was expanded by 3.13 % and showed a constant trend from 2011 to 2021. From 2000 to 2021, there was a consistent upward trend in total carbon emissions within the ellipse. Specifically, the periods of 2000–2006, 2006–2011, 2011–2016, and 2016–2021 had increases of 3.85 %, 73.62 %, 13.24 %, and 17.05 %, respectively. Overall, there was a significant increase of 138.99 % in carbon emissions within the ellipse for the entire period. So, even though the area of the ellipse was expanding, the intensity of carbon emissions that occurred within the ellipse's area also increased.

Standard deviational ellipse can also show the spatial features of carbon emissions based on different classes (Fig. 7). The locations of low and low-moderate classes were relatively the same during the study period, in the western and middle regions, respectively. The locations of moderate, high-moderate, and high ellipses were changing dynamically during 2000–2021. The eastern region of the study area became the center of moderate to high emissions.

The area of each class showed the different phenomenon (Fig. 8). The low class increased significantly in 2006, then declined dramatically in 2011, before continuing on a stable trajectory until 2021. The low-moderate class had a declining trend in 2006, rose in 2011, and then decreased in the subsequent years. The proportion of moderate, high-moderate, and high classes areas showed an expanding trend. During 2000–2021, moderate emission area grew by 330.65 % (from 633 km^2 to 2726 km^2), high-moderate emission area by 297.20 % (from 107 km^2 to 425 km^2), and high emission area by 871.43 % (from 7 km^2 to 68 km^2).

km^2). These phenomena showed that areas with moderate to high emissions classes were expanding in the recent years.

3.3. Eco-environmental quality in Samarinda Metropolitan Area

3.3.1. Principal component analysis (PCA) of RSEICs

Principal Component Analysis (PCA) was performed to understand the role of each indicator in RSEI. The means of RSEICs and weight values of each indicator from the PCA method are shown in Table 3. Means of RSEICs value in selected years show that the mean eco-environmental quality of the Samarinda Metropolitan Area is categorized as inferior (2000), fairly poor (2006, 2011, 2016), and fair (2021). Based on PCA analysis, the contribution rate of PC1 of every study year was $>75\%$ and PC1 was used to indicate the eco-environmental quality of the study area. The contribution rates of PC1 in 2000, 2006, 2011, 2016, and 2021 were 88.89 %, 80.67 %, 79.99 %, 78.71 %, and 82.17 %, respectively.

The load signs show that NDVI, WET, and Csink had positive effects on eco-environmental quality, while LST and NDBSI had the opposite effects (Table 3). The increase in greenness (NDVI), wetness (WET) and Csink can indicate an increase in eco-environmental quality. The increase of heat (LST) and dryness (NDBSI) can indicate the degradation of eco-environmental quality. Csink was the most essential factor of RSEICs, with higher values compared to other indexes weight in each year.

At the city-level, the mean value of RSEICs is depicted in Fig. 9. The mean RSEICs during the time span shows the dynamic of eco-environmental quality at the city level. Kutai Timur had the highest mean RSEICs value in all selected years, with mean value and class in each year: 2000 (0.736338, good), 2006 (0.625583, moderately good),

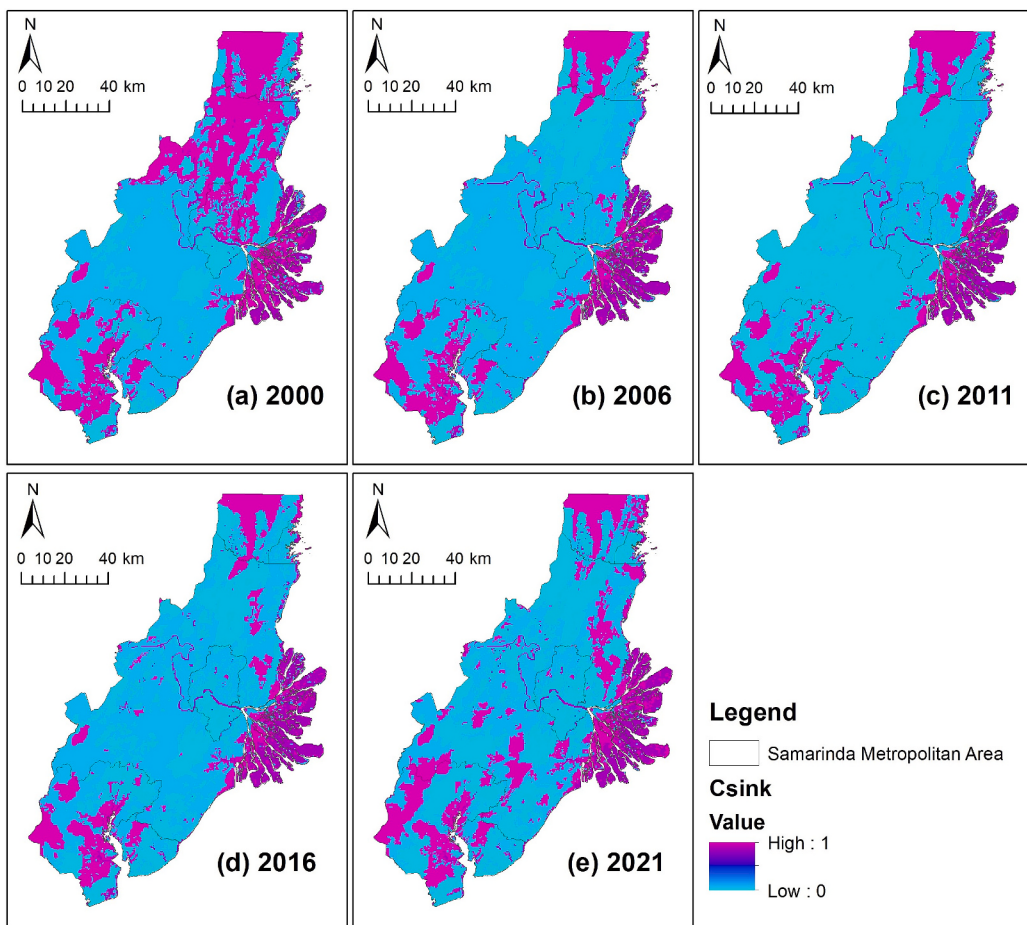


Fig. 14. Spatial distribution of Csink in 2000, 2006, 2011, 2016, and 2021.

2011 (0.622636, moderately good), 2016 (0.491140, inferior), and 2021 (0.565106, moderate). This shows that Kutai Timur has better eco-environmental quality compared to other cities in the region.

On the contrary, the city or municipality with the lowest mean RSEICs value during selected years was: 2000 (Balikpapan, 0.27552), 2006 (Samarinda, 0.109989), 2011 (Samarinda, 0.119063), 2016 (Samarinda, 0.125178), and 2021 (Samarinda, 0.128949). In 2000, Balikpapan's eco-environmental quality was at a fairly poor level. However, in the following years, Samarinda occupied the lowest position, with an eco-environmental quality that was classified as poor. This condition shows that there was a significant decline in the quality of the eco-environment in Samarinda after 2000. This phenomenon occurred because of significant changes in the land use composition of Samarinda city, which initially 80 % was still undeveloped. After 2000, there was a massive increase in the area of settlements and buildings.

3.3.2. Spatial mapping of RSEICs and its indicators

Figs. 10–14 show the dynamic changes of all the indicators of RSEICs in the Samarinda Metropolitan Area during the study period.

The RSEICs map was generated from PCA analysis of five indicators maps. Fig. 15 visualizes the spatial distribution of RSEICs based on classes in the study area. RSEICs map showed that only six classes appeared after the analysis, including: class 1 (very poor), 2 (poor), 3 (fairly poor), 8 (good), 9 (very good), and 10 (excellent). In 2000, there were only four RSEICs classes: 1, 2, 9, and 10. Meanwhile, in 2006 and 2016, there were five classes: 1, 2, 8, 9, and 10. This phenomenon shows that the distribution of RSEICs values tends to be only distributed among these classes. The distribution of RSEICs values reflects the eco-environmental quality at the spatial point (grid) scale was at extreme

level: whether low (1, 2, 3) or high (8, 9, 10).

Table 4 shows the proportion of RSEICs classes in the Samarinda Metropolitan Area from 2000 to 2021. The total area of each year is varied because of the changes in water bodies (eliminated through the water masking process). All RSEICs classes experienced fluctuations during the 2000–2021 period. For the very poor class, when compare 2000 and 2021, the area was decreased from 6896.25 km² to 2556 km². On the contrary, the poor class area was expanded drastically from 375.25 km² to 5767.5 km². For fairly poor and good classes, the area was relatively small compared to other classes. Very good class showed the expanding trend in 2000–2021, from 523.75 km² to 645 km² or equal to 23.15 % increase, while excellent class was declined by 30.28 % (from 4103.75 km² to 2861.25 km²). From this phenomenon, it can be seen that the proportion of areas with very poor and poor classes is greater than very good and excellent classes.

3.3.3. Directional distribution of RSEICs classes

Fig. 16 and Table 5 shows the directional distribution of RSEICs classes and its parameters. The center location of each class in each year was varied. The center location of very poor class was in Kutai Kartanegara (2000, 2011) and Samarinda (2006, 2016, 2021), while poor class was in Penajam Paser Utara (2000) and Kutai Kartanegara (2006, 2011, 2016, 2021). Fairly poor class was located in Penajam Paser Utara (2016, 2021). Good class center was moving dynamically: from Penajam Paser Utara to Kutai Kartanegara and Samarinda. Interestingly, the location of very good class was consistent in the eastern Kutai Kartanegara, which is nearby the coast. Then, the location of excellent class was in Samarinda (2000), then moved to Kutai Kartanegara (2006, 2011, 2016, 2021). The movement of the center indicates the changes in

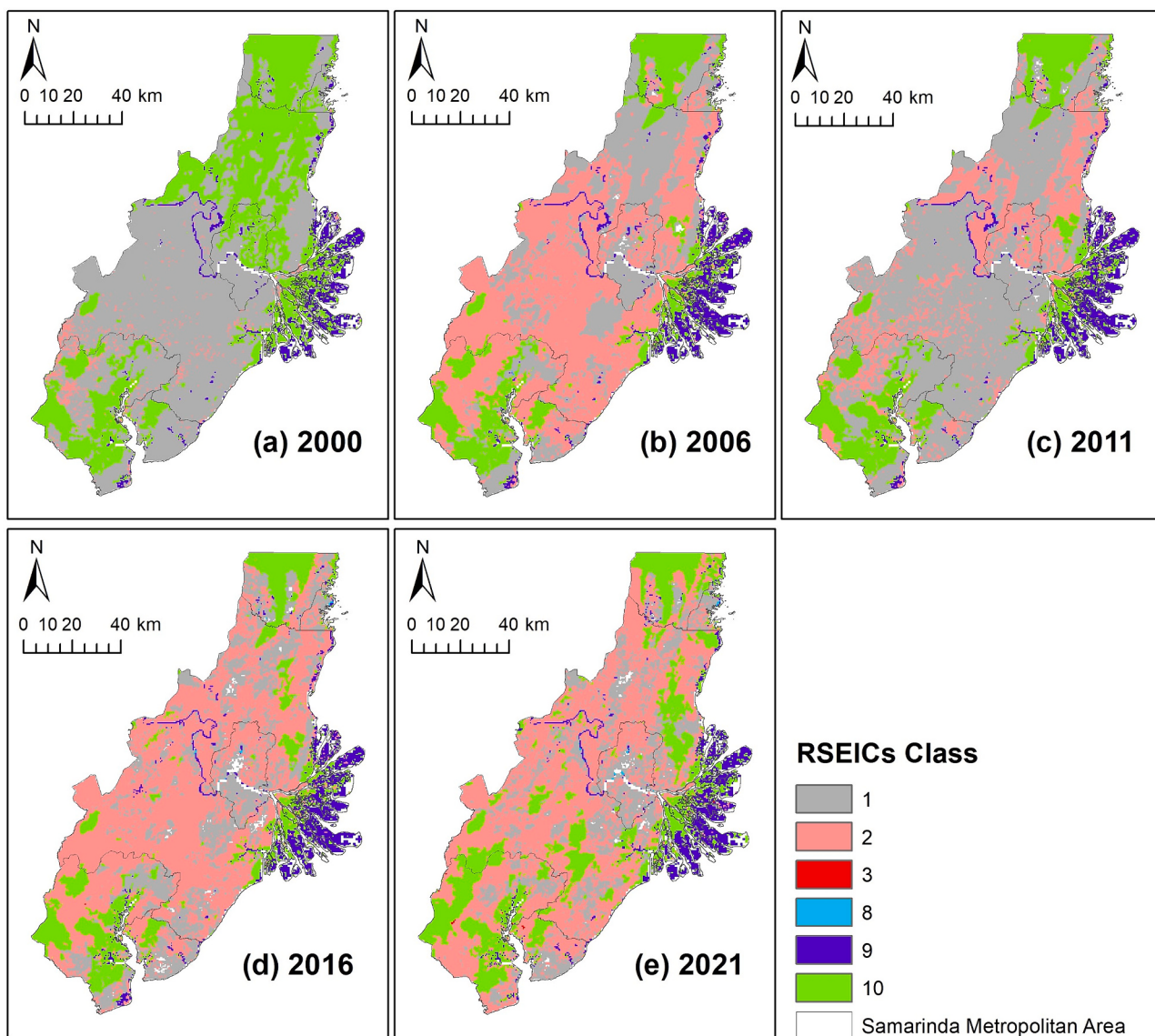


Fig. 15. Spatial distribution of RSEICs in 2000, 2006, 2011, 2016, and 2021.

Table 4
Proportion area of RSEICs based on post-analysis classes.

		RSEICs class					
		1	2	3	8	9	10
2000	Area (km ²)	6896.25	375.25	0.0	0.0	523.75	4103.75
	%	57.96	3.15	0.0	0.0	4.40	34.49
2006	Area (km ²)	3456	5685.75	0.0	0.5	692.75	2039.5
	%	29.10	47.88	0.0	0.004	5.84	17.17
2011	Area (km ²)	6620	2474.75	0.0	2	689.75	2090
	%	55.74	20.84	0.0	0.02	5.81	17.60
2016	Area (km ²)	2973.5	6246.75	0.25	4.5	693	1892.5
	%	25.18	52.89	0.002	0.04	5.87	16.02
2021	Area (km ²)	2556	5767.5	5.5	8.5	645	2861.25
	%	21.58	48.70	0.05	0.07	5.45	24.16

the core area of each RSEICs class during the study period.

The azimuth, X-, and Y-axes of all class ellipses changed in each selected year (Table 5). A comparison between 2000 and 2021 for the very poor class showed that the X-axis decreased by 4.81 km while the Y-axis increased by 4.38 km, which shows a decrease in the dispersion of this class with more obvious northeast-southwest direction in the inland region. During 2000–2021, poor class X-axis declined drastically by

24.61 km, while Y-axis length increased by 43.73 km. The poor class ellipse was extending from southwest region to the northeastern part. This phenomenon shows a shift in eco-environment degradation in the study area from the southern part to the central and northern areas. However, these two classes were consistently located in the inland region.

During the study period, two classes were unable to generate ellipses

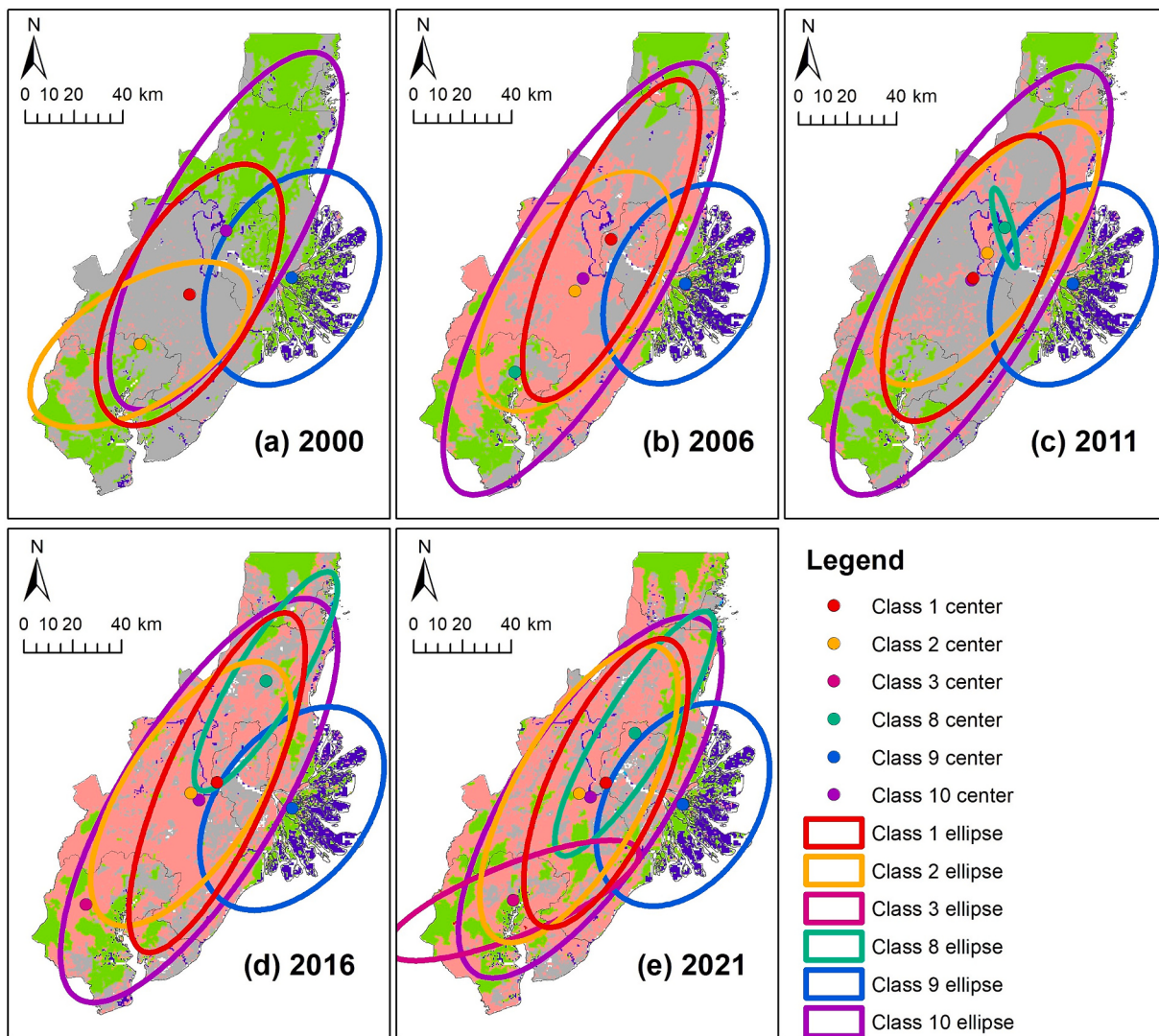


Fig. 16. Directional distribution of RSEICs class in Samarinda Metropolitan Area.

because the grid values belonging to these classes were very minimal, such as the good class in 2006 and the fairly poor class in 2016. However, in 2021, the ellipse for the fairly poor class was located in the south with an azimuth of 68.14° , while the good class ellipse is in the middle to the north with an azimuth of 31.69° . This shows that the fairly poor and good classes did not intersect.

From 2000 to 2021, the very good-class ellipse shows an unchanged location in the coastal area, which is the estuary, with a rotational shift from 28.11° to 32.61° . This condition indicates that the eco-environmental quality in the central coastal area was classified as very good. The excellent class ellipse shows a unique phenomenon because it experiences lengthening of the X-axis and Y-axis simultaneously when compared between 2000 and 2021, namely: 2.58 km and 3.44 km, respectively. The excellent class ellipse shows a shifting trend in environmental quality from north to south. This situation shows that the environmental quality has improved, especially in coastal and mountainous areas in the central and southern parts.

3.4. Dynamic relationship between carbon emissions and eco-environmental quality in Samarinda Metropolitan Area

3.4.1. Coupling status of carbon emissions (CE) and eco-environmental quality (RSEICs)

The dynamic relationship between carbon emissions and eco-

environmental quality can be described by the coupling status. Fig. 17 illustrates the coupling status between CE and RSEICs in the Samarinda Metropolitan Area in 2000, 2006, 2011, 2016, and 2021. The findings indicated that most of the regions in the Samarinda Metropolitan Area have a weak coupling degree (0–0.2). The areas with a slight weak coupling status (0.2–0.4) were distributed in the outer region of built-up areas, mining, agriculture, forests, and several points in coastal areas. As the second largest coupling status, the slight weak coupling status tends to surround the higher coupling degrees. Based on the coupling status map, the areas that have barely balance status, slight strong coupling status, and strong coupling status were mostly concentrated in settlement areas and city centers.

Fig. 18 illustrates the proportion area of different degrees in the study area during selected years. The findings showed that the area of the higher coupling degrees was decreasing. The trend of strong coupling states declined from 349.75 km^2 in 2000 to 245 km^2 in 2021. The same situation also happened to slight strong coupling and barely balance state that were decreasing from 721.75 km^2 (2000) to 241 km^2 (2021) and 1010.25 km^2 (2000) to 832.75 km^2 (2021), respectively. In contrast, the increasing trend was obvious in slight weak coupling. Between 2000 and 2021, the slight weak coupling was expanded by 2570.5 km^2 .

The coupling status of CE and RSEICs in the Samarinda Metropolitan Area showed that there was little direct correlation between carbon

Table 5
Directional distribution parameters of RSEICs class.

Year	RSEICs class	X center coordinate	Y center coordinate	X std. dev. (km)	Y std. dev. (km)	Azimuth/rotation (°)
2000	1	116.97	-0.66	27.63	59.82	29.92
	2	116.79	-0.85	50.83	24.74	58.22
	9	117.35	-0.60	32.47	46.73	28.11
	10	117.11	-0.42	28.53	82.80	29.58
2006	1	117.10	-0.46	21.51	71.70	25.24
	2	116.96	-0.65	28.03	56.57	34.86
	8	116.75	-0.95	-	-	-
	9	117.37	-0.62	29.93	43.53	28.90
2011	10	116.99	-0.60	31.20	100.40	30.01
	1	117.00	-0.60	25.77	64.13	26.78
	2	117.05	-0.51	25.28	65.86	38.49
	8	117.12	-0.41	3.14	16.66	165.00
2016	9	117.37	-0.62	30.12	44.10	29.56
	10	116.99	-0.61	31.12	99.82	30.16
	1	117.08	-0.54	21.33	75.51	23.72
	2	116.98	-0.58	26.72	62.59	33.46
2021	3	116.59	-0.99	-	-	-
	8	117.26	-0.17	12.92	52.11	31.52
	9	117.35	-0.64	30.35	47.37	38.22
	10	117.01	-0.61	32.07	95.28	31.56
2021	1	117.08	-0.55	22.82	64.2	24.48
	2	116.98	-0.59	26.22	68.47	29.41
	3	116.74	-0.98	55.36	14.64	68.14
	8	117.18	-0.36	13.66	58.31	31.69
2021	9	117.36	-0.63	30.59	45.39	32.61
	10	117.02	-0.60	31.11	86.24	33.28

emissions and eco-environmental quality within the majority of the region. Also, the decreasing trend of higher coupling degrees indicates a potential improvement between CE and RSEICs. However, higher coupling degrees that were concentrated in population centers and crucial areas like downtown need to be decreased through urban greening or green infrastructure. Also, the expansion of the higher coupling areas must be prevented so that the areas do not affect the surrounding regions.

3.4.2. CE-RSEICs coupling and existing LULC in Samarinda Metropolitan Area

To understand the relationship between coupling status and existing regional conditions, the land use-land cover (LULC) aspect can be taken into consideration, especially for optimizing regional development. The LULC composition for each coupling status can be seen in Fig. 19.

Based on the results of the CE-RSEICs coupling analysis and its relation to actual conditions, the coupling degree is influenced by the LULC composition. The main composition of each coupling degree was determined by the proportion or percentage of the largest LULC type compared to the total area of each coupling class. The largest LULC proportion for weak coupling in selected years, namely: 2000 (forest, 50.45 %), 2006 (grassland, 45.87 %), 2011 (cropland, 40.54 %), 2016 (grassland, 39.06 %), and 2021 (forest, 45.14 %). The largest LULC types for slight weak coupling are: 2000 (grassland, 94.58 %), 2006 (grassland, 79.49 %), 2011 (cropland, 63.74 %), 2016 (grassland, 49.07 %), and 2021 (cropland, 47.85 %). For barely balance coupling, cropland became the highest composition of LULC in all years: 2000 (56.08 %), 2006 (41.80 %), 2011 (58.38 %), 2016 (34.18 %), and 2021 (40.05 %). The dominance of forest, grassland, and cropland influences the low

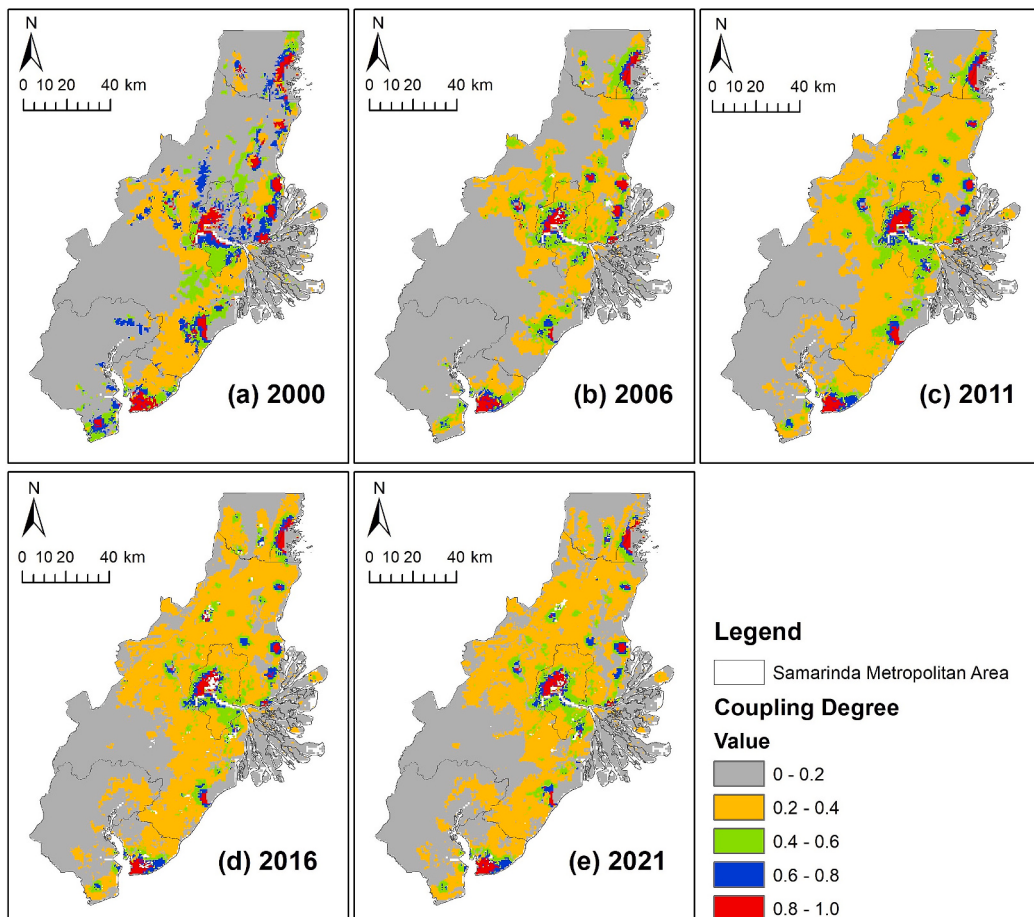


Fig. 17. Coupling status map of CE-RSEICs in Samarinda Metropolitan Area.

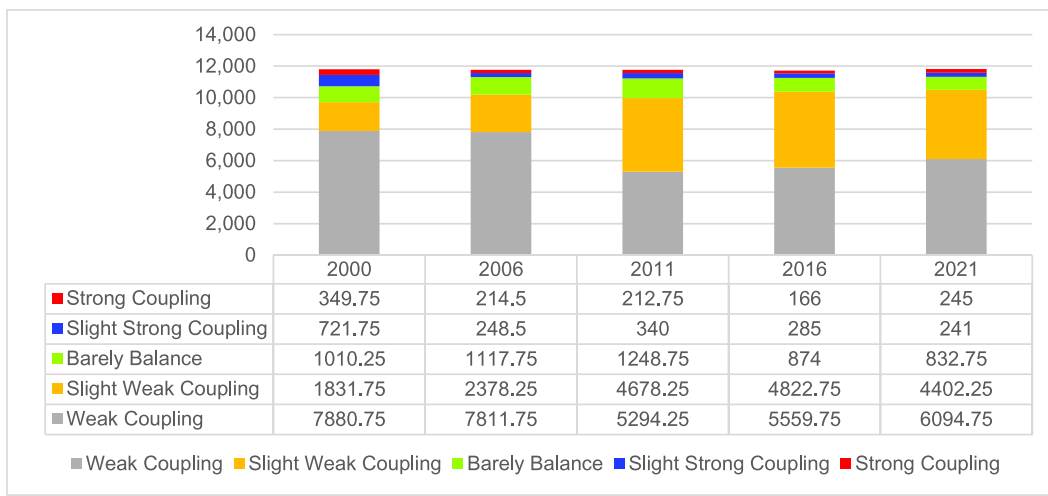
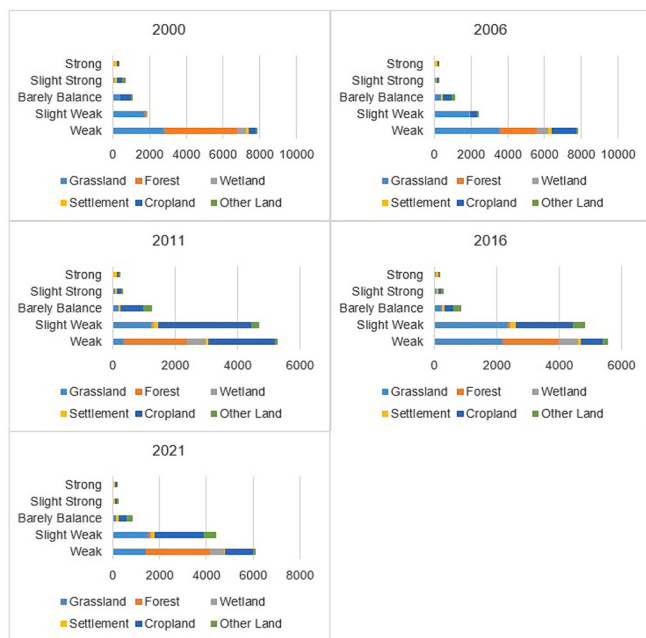
Fig. 18. CE-RSEICs coupling status area (km²).

Fig. 19. Composition of LULC for each coupling degree.

level of correlation between carbon emissions and eco-environmental quality in the region.

The opposite condition was shown in slight strong and strong coupling, because the coupling degree of carbon emissions and eco-environmental quality was starting to strengthen. Interestingly, the largest LULC type in slight strong coupling was cropland, with the percentage of cropland area compared to the total slight strong coupling area in each year: 2000 (43.39 %), 2006 (35.71 %), 2011 (42.57 %), 2016 (33.25 %), and 2021 (32.88 %). However, croplands that have a slight strong coupling were mostly located near settlements or built-up areas. Settlement area occupied the highest percentage when compared to the total strong coupling area in all years: 45.93 %, 51.51 %, 52.41 %, 51.81 %, and 60 % in 2000, 2006, 2011, 2016, and 2021, respectively. Based on these results, the dominance of settlement areas has an impact on increasing the coupling degree of carbon emissions and eco-environmental quality in the study area.

4. Discussions

4.1. Characteristics and interaction of CE-RSEICs in coastal metropolitan area

The coastal region is a crucial area in carbon emissions reduction and environmental quality optimization. With various important and unique elements of the coastal area, the Samarinda Metropolitan Area has special characteristics in terms of carbon emissions and eco-environmental quality. Carbon emissions in the Samarinda metropolitan area show an increasing trend during the 2000–2021 period, with intensity centers distributed along the coast (eastern part) and core cities in the region. This phenomenon is in line with previous studies which show a similar increasing trend of carbon emissions in coastal areas, such as in Indonesia's coastal regions (Arifanti et al., 2021; Eddy et al., 2021; Susetyo Adi et al., 2020), the eastern coastal areas of China (Chuai et al., 2015; Pan et al., 2022), and coastal areas of Southeast Asia and global (Adame et al., 2021; Kirwan et al., 2023; Rosentreter et al., 2023; Stankovic et al., 2021). In previous studies, the trend of increasing emissions in coastal areas is caused by degradation of coastal ecosystems due to land use change, massive development, and the loss of coastal carbon storage (Pendleton et al., 2012; Sejati et al., 2020; Tan et al., 2023).

Based on RSEICs analysis in selected years, the average eco-environmental quality status in the Samarinda metropolitan area is in fairly poor to inferior class. NDVI and WET are positively correlated with eco-environmental quality in the Samarinda Metropolitan Area, where both indicators are able to indicate an increase in the area's eco-environmental quality. These results support previous studies, which also stated that increasing NDVI and WET values will be followed by eco-environmental quality improvement (Jing et al., 2020; Xu et al., 2019; Yang and Li, 2023). Also, this study supports the previous research about NDVI and WET that correlated positively in the warm season (Zhang et al., 2021), which has similarity to the study area (tropical climate and warm season throughout the year). On the other hand, based on this study, LST and NDBSI indicate degradation of eco-environmental quality, which is supported by the results of previous studies that reveal these two indicators have a negative impact on the ecological environment (Cao et al., 2022; Wang et al., 2022; Ye and Kuang, 2022). In the context of RSEICs integration, this study confirms that carbon sinks are also positively correlated with eco-environment quality, with the highest weight value in all selected years. Apart from that, the PC1 contribution level for RSEICs is in the range of 78–89 % and even tends to be stable compared to conventional RSEI with four indicators with a PC1 contribution around 50–80 % (Cao et al., 2022;

Liao et al., 2023; H. Wang et al., 2023; Wang et al., 2022). The novelty of integrating CE-RSEICs in this research can improve conventional RSEI analysis methods, especially in carbon-related research, to support sustainable low-carbon development.

From a spatial perspective, this study enriches the use of the directional distribution (standard deviational ellipse) method in carbon emissions and eco-environmental quality research. In this study, the directional distribution method is applied to each CE and RSEICs class in order to understand more deeply the spatial features at each level. Therefore, this study can complement previous research that used the standard deviational ellipse method by focusing on aggregate or total carbon emissions (Duman et al., 2023; Gui et al., 2023; Lv et al., 2023).

CE-RSEICs in coastal metropolitan areas shows a complex form of interaction. The majority of the study area have weak and slight weak coupling degrees with an increasing trend. Meanwhile, the higher coupling degree shows a decreasing trend, which indicates potential improvement in the ecological environment in the study area. However, higher coupling degrees are concentrated in population centers and settlements, such as urban and coastal areas. This phenomenon is supported by a study in East Kalimantan province, which revealed that in recent years the province has been in good environmental conditions at a macro level, but the high environment vulnerability index is located in urban, coastal, and ex-mining areas as a result of lack of vegetation cover, urban development, and dense population (Kurniawan et al., 2022). Therefore, to overcome the problem of carbon emissions and environmental degradation in coastal areas, it is necessary to consider the existing conditions, especially those related to LULC.

4.2. Research implications

By using a spatiotemporal approach, this study proves that there is a correlation between carbon emissions and eco-environmental quality in the coastal metropolitan area during the 2000–2021 period. This evidence also supports previous studies that explored the relationship between carbon emissions and ecological-environmental quality (An et al., 2023; Chen et al., 2020; Yang and Li, 2023; Zhang et al., 2024). By choosing the Samarinda metropolitan area as a case study, this study can represent the condition of Indonesia's coastal areas, which are still in a rapid development phase, especially in the process of moving the country's capital to East Kalimantan province. The capital relocation not only constructs massive monumental buildings, infrastructure, and facilities but also embodies national identity and becomes the former government's legacy (in this context: President Joko Widodo era) (Hudalah, 2023). This study can contribute as one of the considerations in developing a more sustainable area to support the new capital development in Indonesia.

With the mean value of eco-environmental quality in the Samarinda Metropolitan Area being relatively poor, the central and regional governments need to be concerned about this issue. Apart from that, there are several other important reasons, namely: a) regional carbon emissions trends that continue to increase from year to year; b) lower RSEICs values in core cities (such as Samarinda, Balikpapan, and Bontang); and c) higher CE-RSEICs coupling degrees that are mostly concentrated within built-up or settlement areas and influence the nearby regions. If these things are not addressed, they have the potential to negatively impact the Samarinda Metropolitan Area, including the strategic areas, such as the national capital.

Local governments, including city/district, provincial and central governments, can strive to reduce carbon emissions and improve eco-environmental quality by: a) improving the condition of areas that have low RSEICs values, with greening and water area conservation programs (S. Chen et al., 2023; Zhou et al., 2023) to increase NDVI, WET, and Csink, b) identifying the dominant sources of carbon emissions (Y. Wang et al., 2023), then reduce carbon emissions in the region based on the sources, c) anticipating massive LULC changes in vulnerable areas, such as coastal and forest/natural areas in order to maintain

natural balance and carbon sink (Fang et al., 2022; Fu et al., 2023; Hoque et al., 2021), and d) implementing the principles of sustainable and low carbon development, also energy efficient and environmentally friendly development (Yu, 2014). This study can also be used as material for consideration in the development of other coastal metropolitan areas, not only in Indonesia but also worldwide. Also, the methodological framework and research implications of this study can contribute to deepening theories and practices for low-carbon development that integrate CE-RSEICs on other scales beyond the Samarinda Metropolitan Area.

4.3. Limitation of the study

This research focuses on the use of eco-environmental quality (RSEICs) in the study of carbon emissions, which is still rarely explored, including the coupling degree between the two and its relationship to existing conditions in coastal metropolitan area. Apart from that, this study also uses a spatiotemporal approach that is able to highlight changes, trends, and CE-RSEICs interactions in spatial and temporal spheres. However, this study still has several limitations, including: (a) this study focuses on the ODIAC dataset as the only source of carbon emissions spatial data (downscaling or top-down approach), (b) this study does not consider the seasonal variables, which might influence the four RSEI indicators (heat, dryness, greenness, and wetness), (c) remote sensing image data processed using water masking has the potential to limit the assessment of the land surface in the area. Therefore, future relevant studies could consider these issues.

5. Conclusion

Using a spatiotemporal approach, this study explores the dynamic relationship between carbon emissions (CE) and integrated eco-environmental quality with carbon sink (RSEICs) in the Samarinda Metropolitan Area, Indonesia. The main conclusions based on the research aims of this study, include:

Carbon emissions in the Samarinda Metropolitan Area continued to increase during 2000–2021, with emissions growth of 157.78 %. At the city level, Kutai Kartanegara as the largest area, being the highest contributor to carbon emissions in all years and followed by core cities in the region: Samarinda, Balikpapan and Bontang. Spatially, the intensity of carbon emissions is mostly concentrated in the developed area and has kept expanding in recent years. The center of carbon emissions was mostly in the eastern part and along the coast, while the southwest region was relatively constant with lower emissions. Kutai Timur, Bontang, Samarinda, and Balikpapan experienced a shift towards higher emissions status when comparing 2000 and 2021, while Kutai Kartanegara and Penajam Paser Utara remained in the same status throughout the study period. For directional distribution, low and low-moderate emissions ellipses showed a declining trend. On the contrary, moderate, high-moderate, and high emissions ellipses showed an expanding trend.

The mean value of eco-environmental quality (RSEICs) in the Samarinda Metropolitan Area ranges between 0.2878 to 0.4223, or is categorized as inferior to fair. Greenness (NDVI), wetness (WET), and Csink have a positive impact on eco-environmental quality, while heat (LST) and dryness (NDBSI) have the opposite impact. In other words, NDVI, WET, and Csink can indicate an increase in eco-environmental quality. At the city level, Kutai Timur has better eco-environmental quality compared to other cities, while Samarinda has RSEICs that was classified as poor. All RSEICs classes areas experienced fluctuations during 2000–2021. But the area proportion of very poor and poor classes is larger than very good and excellent classes. Ellipse of RSEICs shows dynamic displacement. The very poor ellipse is located in the inland, while the poor ellipse extends from the southwest to the northeastern part. The very-good class ellipse shows an unchanged location on the eastern coast, and the excellent class ellipse shows a shifting trend of

environmental quality improvement from north to south.

The interaction between carbon emissions and eco-environmental quality is indicated by coupling status. Most of the regions in the Samarinda Metropolitan Area have weak and slight weak coupling degrees, which indicate there is little direct correlation between CE and RSEICs in the majority of the region. However, higher coupling degrees are mostly concentrated in population centers, like settlement areas. In addition, the analysis of the current land use and land cover (LULC) composition in each coupling class reveals that the settlement area has the largest percentage of LULC type composition in the strong coupling class. Additionally, regions in proximity to settlement areas have a greater coupling class in comparison to those that are more distant. Therefore, the settlement area has an impact on increasing the CE-RSEICs coupling degree.

Understanding CE, RSEICs, and the relationship between both variables is crucial for sustainable and low-carbon development, especially in vulnerable areas like coastal regions. This study suggests the integration between carbon issues and eco-environmental quality, as well as considering the spatiotemporal aspects and existing conditions. In the context of urban development, this study also suggests starting the improvement in the areas that have a lower RSEICs value and higher emissions centers, anticipating massive changes in LULC, and maintaining the balance of ecological aspects and carbon sinks.

CRediT authorship contribution statement

Ainun Hasanah: Writing – original draft, Visualization, Software, Methodology, Formal analysis, Data curation, Conceptualization. **Jing Wu:** Writing – review & editing, Validation, Supervision, Methodology, Conceptualization.

Declaration of competing interest

The authors declare that they have no known competing financial interests or personal relationships that could have appeared to influence the work reported in this paper.

Data availability

Data will be made available on request.

Appendix A. Supplementary data

Supplementary data to this article can be found online at <https://doi.org/10.1016/j.scitotenv.2024.172188>.

References

- Acheampong, A.O., Adams, S., Boateng, E., 2019. Do globalization and renewable energy contribute to carbon emissions mitigation in Sub-Saharan Africa? *Sci. Total Environ.* 677, 436–446. <https://doi.org/10.1016/j.scitotenv.2019.04.353>.
- Adame, M.F., Connolly, R.M., Turschwell, M.P., Lovelock, C.E., Fatoyinbo, T., Lagomasino, D., Goldberg, L.A., Holdorf, J., Friess, D.A., Sasmito, S.D., Sanderman, J., Sievers, M., Buelow, C., Kauffman, J.B., Bryan-Brown, D., Brown, C.J., 2021. Future carbon emissions from global mangrove forest loss. *Glob. Chang. Biol.* 27 (12), 2856–2866. <https://doi.org/10.1111/gcb.15571>.
- An, M., Xie, P., He, W., Wang, B., Huang, J., Khanal, R., 2023. Local and tele-coupling development between carbon emission and ecologic environment quality. *J. Clean. Prod.* 394, 136409 <https://doi.org/10.1016/j.jclepro.2023.136409>.
- Arifanti, V.B., Novita, N., Subarno, Tosiani, A., 2021. Mangrove deforestation and CO₂ emissions in Indonesia. *IOP Conference Series: Earth and Environmental Science* 874 (1), 012006. <https://doi.org/10.1088/1755-1315/874/1/012006>.
- Bianco, V., Cascetta, F., Marino, A., Nardini, S., 2019. Understanding energy consumption and carbon emissions in Europe: a focus on inequality issues. *Energy* 170, 120–130. <https://doi.org/10.1016/j.energy.2018.12.120>.
- Boschken, H.L., 2013. Global cities are coastal cities too. *Urban Stud.* 50 (9), 1760–1778 (JSTOR).
- Bukvic, A., Rohat, G., Apotsos, A., De Sherbinin, A., 2020. A systematic review of coastal vulnerability mapping. *Sustainability* 12 (7), 2822. <https://doi.org/10.3390/su12072822>.
- Buotte, P.C., Law, B.E., Ripple, W.J., Berner, L.T., 2020. Carbon sequestration and biodiversity co-benefits of preserving forests in the western United States. *Ecol. Appl.* 30 (2), e02039 <https://doi.org/10.1002/eaap.2039>.
- Cao, J., Wu, E., Wu, S., Fan, R., Xu, L., Ning, K., Li, Y., Lu, R., Xu, X., Zhang, J., Yang, J., Yang, L., Lei, G., 2022. Spatiotemporal dynamics of ecological condition in Qinghai-Tibet Plateau based on remotely sensed ecological index. *Remote Sens.* 14 (17), 4234. <https://doi.org/10.3390/rs14174234>.
- Chandra Voumik, L., Sultana, T., 2022. Impact of urbanization, industrialization, electrification and renewable energy on the environment in BRICS: fresh evidence from novel CS-ARDL model. *Heliyon* 8 (11), e11457. <https://doi.org/10.1016/j.heliyon.2022.e11457>.
- Chen, J., Li, Z., Dong, Y., Song, M., Shahbaz, M., Xie, Q., 2020. Coupling coordination between carbon emissions and the eco-environment in China. *J. Clean. Prod.* 276, 123848 <https://doi.org/10.1016/j.jclepro.2020.123848>.
- Chen, H., Hou, M., Xi, Z., Zhang, X., Yao, S., 2023a. Co-benefits of the National Key Ecological Function Areas in China for carbon sequestration and environmental quality. *Front. Ecol. Evol.* 11, 1093135 <https://doi.org/10.3389/fevo.2023.1093135>.
- Chen, W., Yang, L., Wu, J., Wu, J., Wang, G., Bian, J., Zeng, J., Liu, Z., 2023b. Spatiotemporal characteristics and influencing factors of traditional villages in the Yangtze River Basin a geodetector model. *Herit. Sci.* 11 (1), 111. <https://doi.org/10.1186/s40494-023-00948-x>.
- Chen, S., Zhang, Q., Chen, Y., Zhou, H., Xiang, Y., Liu, Z., Hou, Y., 2023c. Vegetation change and eco-environmental quality evaluation in the loess plateau of China from 2000 to 2020. *Remote Sens.* 15 (2), 424. <https://doi.org/10.3390/rs15020424>.
- Chopra, R., Magazzino, C., Shah, M.I., Sharma, G.D., Rao, A., Shahzad, U., 2022. The role of renewable energy and natural resources for sustainable agriculture in ASEAN countries: do carbon emissions and deforestation affect agriculture productivity? *Res. Policy* 76, 102578. <https://doi.org/10.1016/j.respol.2022.102578>.
- Chuai, X., Huang, X., Wang, W., Zhao, R., Zhang, M., Wu, C., 2015. Land use, total carbon emissions change and low carbon land management in Coastal Jiangsu, China. *J. Clean. Prod.* 103, 77–86. <https://doi.org/10.1016/j.jclepro.2014.03.046>.
- Das, M., Das, A., Pereira, P., 2023. Developing an integrated urban ecological efficiency framework for spatial ecological planning: a case on a tropical mega metropolitan area of the global south. *Geosci. Front.* 14 (1), 101489 <https://doi.org/10.1016/j.gsf.2022.101489>.
- Dogah, K.E., Aworuyi Churchill, S., 2022. Carbon emissions convergence and determinant analysis: evidence from ASEAN countries. *J. Environ. Manag.* 323, 116299 <https://doi.org/10.1016/j.jenvman.2022.116299>.
- Du, X., Shen, L., Wong, S.W., Meng, C., Yang, Z., 2021. Night-time light data based decoupling relationship analysis between economic growth and carbon emission in 289 Chinese cities. *Sustain. Cities Soc.* 73, 103119 <https://doi.org/10.1016/j.scs.2021.103119>.
- Duman, Z., Mao, X., Cai, B., Zhang, Q., Chen, Y., Gao, Y., Guo, Z., 2023. Exploring the spatiotemporal pattern evolution of carbon emissions and air pollution in Chinese cities. *J. Environ. Manag.* 345, 118870 <https://doi.org/10.1016/j.jenvman.2023.118870>.
- Eddy, S., Milantara, N., Sasmito, S.D., Kajita, T., Basyuni, M., 2021. Anthropogenic drivers of mangrove loss and associated carbon emissions in South Sumatra, Indonesia. *Forests* 12 (2), 187. <https://doi.org/10.3390/f12020187>.
- Fang, K., Tang, Y., Zhang, Q., Song, J., Wen, Q., Sun, H., Ji, C., Xu, A., 2019. Will China peak its energy-related carbon emissions by 2030? Lessons from 30 Chinese provinces. *Appl. Energy* 255, 113852. <https://doi.org/10.1016/j.apenergy.2019.113852>.
- Fang, Z., Ding, T., Chen, J., Xue, S., Zhou, Q., Wang, Y., Wang, Y., Huang, Z., Yang, S., 2022. Impacts of land use/land cover changes on ecosystem services in ecologically fragile regions. *Sci. Total Environ.* 831, 154967 <https://doi.org/10.1016/j.scitotenv.2022.154967>.
- Fischer, M.M., Getis, A., (Eds.), 2010. *Handbook of Applied Spatial Analysis: Software Tools, Methods and Applications*. Springer Berlin Heidelberg. <https://doi.org/10.1007/978-3-642-03647-7>.
- Fu, Y., Huang, M., Gong, D., Lin, H., Fan, Y., Du, W., 2023. Dynamic simulation and prediction of carbon storage based on land use/land cover change from 2000 to 2040: a case study of the Nanchang urban agglomeration. *Remote Sens.* 15 (19), 4645. <https://doi.org/10.3390/rs15194645>.
- Griffin, P.W., Hammond, G.P., Norman, J.B., 2016. Industrial energy use and carbon emissions reduction: a UK perspective. *WIREs Energy and Environment* 5 (6), 684–714. <https://doi.org/10.1002/wene.212>.
- Griggs, G., Reguero, B.G., 2021. Coastal adaptation to climate change and sea-level rise. *Water* 13 (16), 2151. <https://doi.org/10.3390/w13162151>.
- Gui, D., He, H., Liu, C., Han, S., 2023. Spatio-temporal dynamic evolution of carbon emissions from land use change in Guangdong Province, China, 2000–2020. *Ecol. Indic.* 156, 111131 <https://doi.org/10.1016/j.ecolind.2023.111131>.
- Hasanah, A., Wu, J., 2023. Spatial and socioeconomic characteristics of CO₂ emissions and sequestration in Indonesian cities. *Heliyon* 9 (11), e22000. <https://doi.org/10.1016/j.heliyon.2023.e22000>.
- Hoque, M.Z., Cui, S., Islam, I., Xu, L., Ding, S., 2021. Dynamics of plantation forest development and ecosystem carbon storage change in coastal Bangladesh. *Ecol. Indic.* 130, 107954 <https://doi.org/10.1016/j.ecolind.2021.107954>.
- Hu, X., Xu, H., 2018. A new remote sensing index for assessing the spatial heterogeneity in urban ecological quality: a case from Fuzhou City, China. *Ecol. Indic.* 89, 11–21. <https://doi.org/10.1016/j.ecolind.2018.02.006>.
- Hudalah, D., 2023. Building a capital city, carving out a megaproject legacy? *Habitat Int.* 141, 102933 <https://doi.org/10.1016/j.habitatint.2023.102933>.

- Jin, T., Kim, J., 2018. What is better for mitigating carbon emissions – renewable energy or nuclear energy? A panel data analysis. *Renew. Sust. Energ. Rev.* 91, 464–471. <https://doi.org/10.1016/j.rser.2018.04.022>.
- Jin, W., Li, H., Wang, J., Zhao, L., Li, X., Fan, W., Chen, J., 2023. Continuous remote sensing ecological index (CRSEI): a novel approach for multitemporal monitoring of eco-environmental changes on large scale. *Ecol. Indic.* 154, 110739 <https://doi.org/10.1016/j.ecolind.2023.110739>.
- Jing, Y., Zhang, F., He, Y., Kung, H., Johnson, V.C., Arikena, M., 2020. Assessment of spatial and temporal variation of ecological environment quality in Ebinur Lake Wetland National Nature Reserve, Xinjiang, China. *Ecol. Indic.* 110, 105874 <https://doi.org/10.1016/j.ecolind.2019.105874>.
- Kirwan, M.L., Megonigal, J.P., Noyce, G.L., Smith, A.J., 2023. Geomorphic and ecological constraints on the coastal carbon sink. *Nature Reviews Earth & Environment* 4 (6), 393–406. <https://doi.org/10.1038/s43017-023-00429-6>.
- Kurniawan, R., Saputra, A.M.W., Wijayanto, A.W., Caesarendra, W., 2022. Eco-environment vulnerability assessment using remote sensing approach in East Kalimantan, Indonesia. *Remote Sensing Applications: Society and Environment* 27, 100791. <https://doi.org/10.1016/j.rsase.2022.100791>.
- Li, J., Zhang, D., Su, B., 2019. The impact of social awareness and lifestyles on household carbon emissions in China. *Ecol. Econ.* 160, 145–155. <https://doi.org/10.1016/j.ecolecon.2019.02.020>.
- Li, R., Wang, Q., Liu, Y., Jiang, R., 2021. Per-capita carbon emissions in 147 countries: the effect of economic, energy, social, and trade structural changes. *Sustainable Production and Consumption* 27, 1149–1164. <https://doi.org/10.1016/j.spc.2021.02.031>.
- Li, R., Li, L., Wang, Q., 2022. The impact of energy efficiency on carbon emissions: evidence from the transportation sector in Chinese 30 provinces. *Sustain. Cities Soc.* 82, 103880 <https://doi.org/10.1016/j.scs.2022.103880>.
- Li, W., An, M., Wu, H., An, H., Huang, J., Khanal, R., 2023. The local coupling and telecoupling of urbanization and ecological environment quality based on multisource remote sensing data. *J. Environ. Manag.* 327, 116921 <https://doi.org/10.1016/j.jenvman.2022.116921>.
- Liao, Y., Wu, G., Zhang, Z., 2023. Multi-scale remote sensing assessment of ecological environment quality and its driving factors in watersheds: a case study of Huashan Creek watershed in China. *Remote Sens.* 15 (24), 5633. <https://doi.org/10.3390/rs15245633>.
- Liú, Z., Deng, Z., Davis, S.J., Giron, C., Ciais, P., 2022. Monitoring global carbon emissions in 2021. *Nature Reviews Earth & Environment* 3 (4), 217–219. <https://doi.org/10.1038/s43017-022-00285-w>.
- Lobser, S.E., Cohen, W.B., 2007. MODIS tasseled cap: land cover characteristics expressed through transformed MODIS data. *Int. J. Remote Sens.* 28 (22), 5079–5101. <https://doi.org/10.1080/01431160701253303>.
- Long, Y., Jiang, F., Deng, M., Wang, T., Sun, H., 2023. Spatial-temporal changes and driving factors of eco-environmental quality in the Three-North region of China. *J. Arid. Land* 15 (3), 231–252. <https://doi.org/10.1007/s40333-023-0053-0>.
- Luqman, M., Rayner, P.J., Gurney, K.R., 2023. On the impact of urbanisation on CO₂ emissions. *Npj Urban Sustainability* 3 (1), 6. <https://doi.org/10.1038/s42949-023-00084-2>.
- Lv, T., Hu, H., Xie, H., Zhang, X., Wang, L., Shen, X., 2023. An empirical relationship between urbanization and carbon emissions in an ecological civilization demonstration area of China based on the STIRPAT model. *Environ. Dev. Sustain.* 25 (3), 2465–2486. <https://doi.org/10.1007/s10668-022-02144-6>.
- Moyer, J.D., 2023. Modeling transformational policy pathways on low growth and negative growth scenarios to assess impacts on socioeconomic development and carbon emissions. *Sci. Rep.* 13 (1), 15996 <https://doi.org/10.1038/s41598-023-42782-y>.
- Oda, T., Maksyutov, S., 2011. A very high-resolution (1 km×1 km) global fossil fuel CO₂ emission inventory derived using a point source database and satellite observations of nighttime lights. *Atmos. Chem. Phys.* 11 (2), 543–556. <https://doi.org/10.5194/acp-11-543-2011>.
- Oda, T., Maksyutov, S., Andres, R.J., 2018. The Open-source Data Inventory for Anthropogenic CO₂, version 2016 (ODIAC2016): a global monthly fossil fuel CO₂ gridded emissions data product for tracer transport simulations and surface flux inversions. *Earth System Science Data* 10 (1), 87–107. <https://doi.org/10.5194/essd-10-87-2018>.
- Oda, T., Bun, R., Kinakh, V., Topylko, P., Halushchak, M., Marland, G., Lauvaux, T., Jonas, M., Maksyutov, S., Nahorski, Z., Lesiv, M., Danylo, O., Horabik-Pyzel, J., 2019. Errors and uncertainties in a gridded carbon dioxide emissions inventory. *Mitig. Adapt. Strateg. Glob. Chang.* 24 (6), 1007–1050. <https://doi.org/10.1007/s11027-019-09877-2>.
- Pan, L., Yu, J., Lin, L., 2022. The temporal and spatial pattern evolution of land-use carbon emissions in China coastal regions and its response to green economic development. *Front. Environ. Sci.* 10, 1018372 <https://doi.org/10.3389/fenvs.2022.1018372>.
- Pendleton, L., Donato, D.C., Murray, B.C., Crooks, S., Jenkins, W.A., Sifleet, S., Craft, C., Fourqurean, J.W., Kauffman, J.B., Marbà, N., Megonigal, P., Pidgeon, E., Herr, D., Gordon, D., Baldera, A., 2012. Estimating global “blue carbon” emissions from conversion and degradation of vegetated coastal ecosystems. *PLoS One* 7 (9), e43542. <https://doi.org/10.1371/journal.pone.0043542>.
- Permadi, D.A., Sofyan, A., Kim Oanh, N.T., 2017. Assessment of emissions of greenhouse gases and air pollutants in Indonesia and impacts of national policy for elimination of kerosene use in cooking. *Atmos. Environ.* 154, 82–94. <https://doi.org/10.1016/j.atmosenv.2017.01.041>.
- Raihan, A., Tuspekova, A., 2022. Toward a sustainable environment: Nexus between economic growth, renewable energy use, forested area, and carbon emissions in Malaysia. *Resources, Conservation & Recycling* 15, 200096. <https://doi.org/10.1016/j.rcradv.2022.200096>.
- Ren, Y., Ren, X., Hu, J., 2019. Driving factors of China’s city-level carbon emissions from the perspective of spatial spillover effect. *Carbon Management* 10 (6), 551–566. <https://doi.org/10.1080/17583004.2019.1676096>.
- Rosentreter, J.A., Laruelle, G.G., Bangs, H.W., Bianchi, T.S., Busecke, J.J.M., Cai, W.-J., Eyre, B.D., Forbrich, I., Kwon, E.Y., Maavara, T., Moosdorf, N., Najjar, R.G., Sarma, V.V.S.S., Van Dam, B., Regnier, P., 2023. Coastal vegetation and estuaries are collectively a greenhouse gas sink. *Nat. Clim. Chang.* 13 (6), 579–587. <https://doi.org/10.1038/s41558-023-01682-9>.
- Saidi, K., Omri, A., 2020. The impact of renewable energy on carbon emissions and economic growth in 15 major renewable energy-consuming countries. *Environ. Res.* 186, 109567 <https://doi.org/10.1016/j.envres.2020.109567>.
- Sejati, A.W., Buchori, I., Kurniawati, S., Brana, Y.C., Fariha, T.I., 2020. Quantifying the impact of industrialization on blue carbon storage in the coastal area of Metropolitan Semarang, Indonesia. *Appl. Geogr.* 124, 102319 <https://doi.org/10.1016/j.apgeog.2020.102319>.
- Shen, S., Wu, C., Gai, Z., Fan, C., 2023. Analysis of the spatiotemporal evolution of the net carbon sink efficiency and its influencing factors at the city level in three major urban agglomerations in China. *Int. J. Environ. Res. Public Health* 20 (2), 1166. <https://doi.org/10.3390/ijerph20021166>.
- Stankovic, M., Ambo-Rappe, R., Carly, F., Dangan-Galon, F., Fortes, M.D., Hossain, M.S., Kiswara, W., Van Luong, C., Minh-Thu, P., Mishra, A.K., Noirkasr, T., Nurdin, N., Panyawai, J., Rattanachot, E., Rozaimi, M., Soe Htun, U., Prathep, A., 2021. Quantification of blue carbon in seagrass ecosystems of Southeast Asia and their potential for climate change mitigation. *Sci. Total Environ.* 783, 146858 <https://doi.org/10.1016/j.scitotenv.2021.146858>.
- Susetyo Adi, N., Sumiran Paputungan, M., Rustam, A., Harjuno Condro Haditomo, A., Medrilzam, 2020. Estimating carbon emission and baseline for blue carbon ecosystems in Indonesia. *IOP Conference Series: Earth and Environmental Science* 530 (1), 012030. <https://doi.org/10.1088/1755-1315/530/1/012030>.
- Tache, A.-V., Popescu, O.-C., Petrișor, A.-I., 2023. Conceptual model for integrating the green-blue infrastructure in planning using geospatial tools: case study of Bucharest, Romania Metropolitan Area. *Land* 12 (7), 1432. <https://doi.org/10.3390/land12071432>.
- Tan, L.-S., Ge, Z.-M., Li, S.-H., Zhou, K., Lai, D.Y.F., Temmerman, S., Dai, Z.-J., 2023. Impacts of land-use change on carbon dynamics in China’s coastal wetlands. *Sci. Total Environ.* 890, 164206 <https://doi.org/10.1016/j.scitotenv.2023.164206>.
- Tang, P., Huang, J., Zhou, H., Fang, C., Zhan, Y., Huang, W., 2021. Local and telecoupling coordination degree model of urbanization and the eco-environment based on RS and GIS: a case study in the Wuhan urban agglomeration. *Sustain. Cities Soc.* 75, 103405 <https://doi.org/10.1016/j.scs.2021.103405>.
- Tian, S., Wang, S., Bai, X., Luo, G., Li, Q., Yang, Y., Hu, Z., Li, C., Deng, Y., 2021. Global patterns and changes of carbon emissions from land use during 1992–2015. *Environmental Science and Ecotechnology* 7, 100108. <https://doi.org/10.1016/j.ese.2021.100108>.
- Wang, G., Han, Q., De Vries, B., 2020. A geographic carbon emission estimating framework on the city scale. *J. Clean. Prod.* 244, 118793 <https://doi.org/10.1016/j.jclepro.2019.118793>.
- Wang, W.-Z., Liu, L.-C., Liao, H., Wei, Y.-M., 2021. Impacts of urbanization on carbon emissions: an empirical analysis from OECD countries. *Energy Policy* 151, 112171. <https://doi.org/10.1016/j.enpol.2021.112171>.
- Wang, X., Yao, X., Jiang, C., Duan, W., 2022. Dynamic monitoring and analysis of factors influencing ecological environment quality in northern Anhui, China, based on the Google Earth Engine. *Sci. Rep.* 12 (1), 20307 <https://doi.org/10.1038/s41598-022-24413-0>.
- Wang, Z., Chen, T., Zhu, D., Jia, K., Plaza, A., 2023a. RSEIFE: a new remote sensing ecological index for simulating the land surface eco-environment. *J. Environ. Manag.* 326, 116851 <https://doi.org/10.1016/j.jenvman.2022.116851>.
- Wang, Y., Jeong, S., Hang, Y., Wang, Q., 2023b. Determinants of net energy-related CO₂ emissions in China: a source-to-sink decomposition analysis. *Environ. Impact Assess. Rev.* 98, 106979 <https://doi.org/10.1016/j.eiar.2022.106979>.
- Wang, Q., Li, L., Li, R., 2023c. Uncovering the impact of income inequality and population aging on carbon emission efficiency: an empirical analysis of 139 countries. *Sci. Total Environ.* 857, 159508 <https://doi.org/10.1016/j.scitotenv.2022.159508>.
- Wang, H., Liu, C., Zang, F., Liu, Y., Chang, Y., Huang, G., Fu, G., Zhao, C., Liu, X., 2023d. Remote sensing-based approach for the assessing of ecological environmental quality variations using Google Earth Engine: a case study in the Qilian Mountains, Northwest China. *Remote Sens.* 15 (4), 960. <https://doi.org/10.3390/rs15040960>.
- Wang, X., Zhang, S., Zhao, X., Shi, S., Xu, L., 2023e. Exploring the relationship between the eco-environmental quality and urbanization by utilizing Sentinel and Landsat data: a case study of the Yellow River Basin. *Remote Sens.* 15 (3), 743. <https://doi.org/10.3390/rs15030743>.
- Wu, L., Zhang, Y., Luo, G., Chen, D., Yang, D., Yang, Y., Tian, F., 2023. Characteristics of vegetation carbon sink carrying capacity and restoration potential of China in recent 40 years. *Frontiers in Forests and Global Change* 6, 1266688. <https://doi.org/10.3389/ffgc.2023.1266688>.
- Xia, C., Li, Y., Xu, T., Chen, Q., Ye, Y., Shi, Z., Liu, J., Ding, Q., Li, X., 2019. Analyzing spatial patterns of urban carbon metabolism and its response to change of urban size: a case of the Yangtze River Delta, China. *Ecol. Indic.* 104, 615–625. <https://doi.org/10.1016/j.ecolind.2019.05.031>.
- Xu, H., Wang, M., Shi, T., Guan, H., Fang, C., Lin, Z., 2018. Prediction of ecological effects of potential population and impervious surface increases using a remote sensing based ecological index (RSEI). *Ecol. Indic.* 93, 730–740. <https://doi.org/10.1016/j.ecolind.2018.05.055>.

- Xu, H., Wang, Y., Guan, H., Shi, T., Hu, X., 2019. Detecting ecological changes with a remote sensing based ecological index (RSEI) produced time series and change vector analysis. *Remote Sens.* 11 (20), 2345. <https://doi.org/10.3390/rs11202345>.
- Yang, Y., Li, H., 2023. Spatiotemporal dynamic decoupling states of eco-environmental quality and land-use carbon emissions: a case study of Qingdao City, China. *Ecological Informatics* 75, 101992. <https://doi.org/10.1016/j.ecoinf.2023.101992>.
- Yang, Y., Li, H., Qian, C., 2023. Analysis of the implementation effects of ecological restoration projects based on carbon storage and eco-environmental quality: a case study of the Yellow River Delta, China. *J. Environ. Manag.* 340, 117929 <https://doi.org/10.1016/j.jenvman.2023.117929>.
- Ye, X., Kuang, H., 2022. Evaluation of ecological quality in Southeast Chongqing based on modified remote sensing ecological index. *Sci. Rep.* 12 (1), 15694 <https://doi.org/10.1038/s41598-022-19851-9>.
- Yin, C., Zhao, W., Ye, J., Muroki, M., Pereira, P., 2023. Ecosystem carbon sequestration service supports the Sustainable Development Goals progress. *J. Environ. Manag.* 330, 117155 <https://doi.org/10.1016/j.jenvman.2022.117155>.
- Yu, L., 2014. Low carbon eco-city: new approach for Chinese urbanisation. *Habitat Int.* 44, 102–110. <https://doi.org/10.1016/j.habitatint.2014.05.004>.
- Yue, H., Liu, Y., Li, Y., Lu, Y., 2019. Eco-environmental quality assessment in China's 35 major cities based on remote sensing ecological index. *IEEE Access* 7, 51295–51311. <https://doi.org/10.1109/ACCESS.2019.2911627>.
- Zerbe, K., Polit, C., McClain, S., Cook, T., 2022. Optimized hot spot and directional distribution analyses characterize the spatiotemporal variation of large wildfires in Washington, USA, 1970–2020. *Int. J. Disaster Risk Sci.* 13 (1), 139–150. <https://doi.org/10.1007/s13753-022-00396-4>.
- Zhang, H., Li, S., 2022. Carbon emissions' spatial-temporal heterogeneity and identification from rural energy consumption in China. *J. Environ. Manag.* 304, 114286 <https://doi.org/10.1016/j.jenvman.2021.114286>.
- Zhang, Y., Wang, Y., Fu, B., Li, M., Lu, Y., Dixit, A.M., Chaudhary, S., Wang, S., 2020. Changes in cultivated land patterns and driving forces in the Three Gorges Reservoir area, China, from 1992 to 2015. *J. Mt. Sci.* 17 (1), 203–215. <https://doi.org/10.1007/s11629-019-5375-1>.
- Zhang, T., Yang, R., Yang, Y., Li, L., Chen, L., 2021. Assessing the urban eco-environmental quality by the remote-sensing ecological index: application to Tianjin, North China. *ISPRS Int. J. Geo Inf.* 10 (7), 475. <https://doi.org/10.3390/jig10070475>.
- Zhang, H., Feng, Z., Shen, C., Li, Y., Feng, Z., Zeng, W., Huang, G., 2022. Relationship between the geographical environment and the forest carbon sink capacity in China based on an individual-tree growth-rate model. *Ecol. Indic.* 138, 108814 <https://doi.org/10.1016/j.ecolind.2022.108814>.
- Zhang, X., Fan, H., Hou, H., Xu, C., Sun, L., Li, Q., Ren, J., 2024. Spatiotemporal evolution and multi-scale coupling effects of land-use carbon emissions and ecological environmental quality. *Sci. Total Environ.* 922, 171149 <https://doi.org/10.1016/j.scitotenv.2024.171149>.
- Zhao, R., Min, N., Geng, Y., He, Y., 2017. Allocation of carbon emissions among industries/sectors: an emissions intensity reduction constrained approach. *J. Clean. Prod.* 142, 3083–3094. <https://doi.org/10.1016/j.jclepro.2016.10.159>.
- Zhao, D., Cai, J., Xu, Y., Liu, Y., Yao, M., 2023a. Carbon sinks in urban public green spaces under carbon neutrality: a bibliometric analysis and systematic literature review. *Urban For. Urban Green.* 86, 128037 <https://doi.org/10.1016/j.ufug.2023.128037>.
- Zhao, N., Wang, K., Yuan, Y., 2023b. Toward the carbon neutrality: forest carbon sinks and its spatial spillover effect in China. *Ecol. Econ.* 209, 107837 <https://doi.org/10.1016/j.jecolecon.2023.107837>.
- Zhou, S., Li, W., Zhang, W., Wang, Z., 2023. The assessment of the spatiotemporal characteristics of the eco-environmental quality in the Chishui River basin from 2000 to 2020. *Sustainability* 15 (4), 3695. <https://doi.org/10.3390/su15043695>.
- Zhu, D., Chen, T., Wang, Z., Niu, R., 2021. Detecting ecological spatial-temporal changes by remote sensing ecological index with local adaptability. *J. Environ. Manag.* 299, 113655 <https://doi.org/10.1016/j.jenvman.2021.113655>.
- Zhu, Q., Guo, X., Guo, J., Wu, J., Ye, Y., Cai, W., Liu, S., 2022. The quality attribute of watershed ecosystem is more important than the landscape attribute in controlling erosion of red soil in southern China. *International Soil and Water Conservation Research* 10 (3), 507–517. <https://doi.org/10.1016/j.iswcr.2021.11.004>.